

Accepted Manuscript

Discovery of potential anticancer multi-targeted ligustrazine based cyclohexanone and oxime analogs overcoming the cancer multidrug resistance

Gao-Feng Zha, Hua-Li Qin, Bahaa G.M. Youssif, Muhammad Wahab Amjad, Maria Abdul Ghafoor Raja, Ahmed H. Abdelazeem, Syed Nasir Abbas Bukhari



PII: S0223-5234(17)30282-9

DOI: [10.1016/j.ejmech.2017.04.025](https://doi.org/10.1016/j.ejmech.2017.04.025)

Reference: EJMECH 9372

To appear in: *European Journal of Medicinal Chemistry*

Received Date: 1 February 2017

Revised Date: 6 April 2017

Accepted Date: 11 April 2017

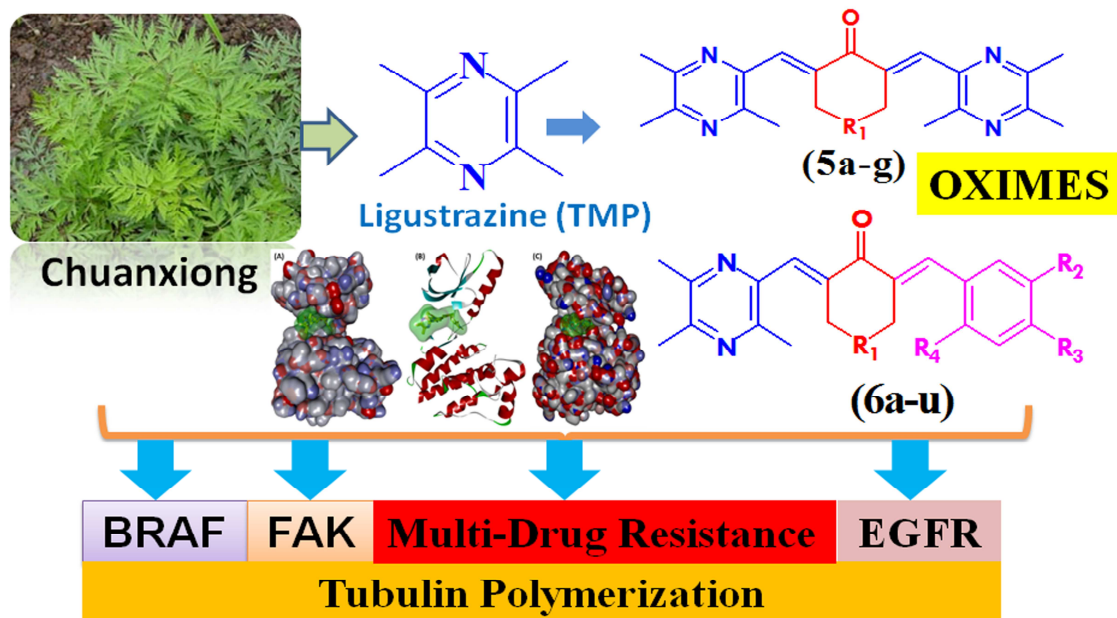
Please cite this article as: G.-F. Zha, H.-L. Qin, B.G.M. Youssif, M.W. Amjad, M.A.G. Raja, A.H. Abdelazeem, S.N.A. Bukhari, Discovery of potential anticancer multi-targeted ligustrazine based cyclohexanone and oxime analogs overcoming the cancer multidrug resistance, *European Journal of Medicinal Chemistry* (2017), doi: 10.1016/j.ejmech.2017.04.025.

This is a PDF file of an unedited manuscript that has been accepted for publication. As a service to our customers we are providing this early version of the manuscript. The manuscript will undergo copyediting, typesetting, and review of the resulting proof before it is published in its final form. Please note that during the production process errors may be discovered which could affect the content, and all legal disclaimers that apply to the journal pertain.

Graphical abstract:

Discovery of potential anticancer multi-targeted ligustrazine based cyclohexanone and oxime analogs overcoming the cancer multidrug resistance

Gao-Feng Zha, Hua-Li Qin, Bahaa G. M. Youssif, Muhammad Wahab Amjad, Maria Abdul Ghafoor Raja, Ahmed H. Abdelazeem, Syed Nasir Abbas Bukhari



Discovery of potential anticancer multi-targeted ligustrazine based cyclohexanone and oxime analogs overcoming the cancer multidrug resistance

Gao-Feng Zha^{a,†}, Hua-Li Qin^{*a}, Bahaa G. M. Youssif^{b,c}, Muhammad Wahab Amjad^d, Maria Abdul Ghafoor Raja^d, Ahmed H. Abdelazeem^{e,f}, Syed Nasir Abbas Bukhari^{*a,b,†}

^a Department of Pharmaceutical Engineering, School of chemistry, chemical engineering and life science, Wuhan University of Technology, 205 Luoshi Road, Wuhan, 430070, P.R.China.

^b Department of Pharmaceutical Chemistry, College of Pharmacy, Aljouf University, Aljouf, Sakaka 2014, Saudi Arabia.

^c Department of Pharmaceutical Organic Chemistry, Faculty of Pharmacy, Assiut University, Assiut 71526, Egypt.

^d College of Pharmacy, Northern Border University, King Abdullah Road, Rafha, Saudi Arabia

^e Department of Medicinal Chemistry, Faculty of pharmacy, Beni-Suef University, Beni-Suef 62514, Egypt.

^f Department of Pharmaceutical Chemistry, College of Pharmacy, Taif University, Taif 21974, Saudi Arabia.

[†]These authors contributed equally

* Authors to whom correspondence should be addressed;

Hua-Li Qin: qinhuali@whut.edu.cn; Syed Nasir Abbas Bukhari: snab_hussaini@yahoo.com;

Abstract

The drug research and development nowadays is focusing on multi-target drugs. In the treatment of cancer, therapies using drugs inhibiting one numerous targets signify a novel viewpoint. In comparison with traditional therapy, multi-targeted drugs directly aim cell subpopulations which are involved in progression of tumor. The current study comprises the synthesis of 34 novel ligustrazine-containing α , β -unsaturated carbonyl-based compounds and oximes. The growth of 5 various cancer cell types was strongly inhibited by ligustrazine-containing oximes as revealed by biological evaluation. A strong SAR was provided by the antiproliferative activity. The mechanistic effects of most active antiproliferative compounds on tubulin polymerization, EGFR TK kinases, KAF and BRAF^{V600E} were investigated, followed by *in vitro* investigation of reversal of efflux-based resistance developed by cancer cells. EGFR was strongly inhibited by two oximes **7e** and **8o**. Out of all linkers including positive control, 1-Isopropyl-piperidin-4-one linker-bearing compounds showed best inhibition of FAK. The strongest inhibitory activity of BRAF^{V600E} was showed by compound **5e** with an IC₅₀ of 0.7 μ M. Analogs such as **5** and **7 (b,e,f)** exhibited a dual role as anticancer as well as MDR reversal agents. For understanding the target protein integrations with new compounds, molecular docking studies were also carried out.

Keywords: Epidermal growth factor receptor (EGFR), BRAF, Focal adhesion kinase (FAK), Tubulin polymerization, Cancer cell lines.

ABBREVIATIONS

MDR , multidrug resistance; EGFR , epidermal growth factor receptor; European Medicines Evaluation Agency (EMA); US Food and Drug Administration (FDA); NSCLC, non-small cell lung; focal adhesion kinase (FAK); RTK , receptor tyrosine kinases; MAPK, mitogen-activated protein kinase; ABC, ATP-binding cassette, NF- κ B, NF-kappaB; Four-point-one, ezrin, radixin, moesin (FERM); Ligustrazine or tetramethylpyrazine (TMP); Adriamycin (Adr); DRS, death receptors; tumor necrosis factor (TNF), PI, propidium iodide; TKIs, tyrosine kinase inhibitors; FAR , fluorescence activity ratio; HRMS, high resolution mass spectra; TLC, thin layer chromatography; UV, ultraviolet; DMEM, Dulbecco's modified Eagle's medium; DMSO, dimethyl sulfoxide; 2-iodoxybenzoic acid (IBX).

INTRODUCTION

After heart disease, cancer is the second most common cause of death, as per statistics [1]. The past few decades have witnessed cancer as a global killer [2]. The antiangiogenic, pro-apoptotic, anti-proliferative and antioxidant properties mediated by multiple signaling pathways are the primary mechanisms of tumor development and progression [3]. To selectively target tubulin polymerization and oncogenically-activated kinases, considerable efforts have been made to discover small molecule inhibitors. To treat HER-2, EGFR and BRAF-driven cancers, a range of inhibitors has been developed such as lapatinib, gefitinib, erlotinib and vemurafenib. Up till now, their effectiveness is restricted to subcategories of oncogenic alterations and majority of kinase inhibitors might not be active against all activating mutations for a particular target.

It has been discovered lately that nearly all patients suffering from hairy-cell leukemia carry the BRAF^{V600E} mutation and the enzyme inhibition resulted in substantial reduction of disease [4]. These discoveries have motivated the researchers to search for small molecule inhibitors aiming the kinase activity of BRAF mutants (particularly BRAF^{V600E}) [5, 6]. For the treatment of BRAF-mutated metastatic melanoma, European Medicines Evaluation Agency (EMA) and US Food and Drug Administration (FDA) have recently approved BRAF-specific inhibitors including dabrafenib (GSK2118436, GSK) and vemurafenib (Zelboraf, Roche), and numerous other BRAF inhibitors are undergoing development stages [7]. Epidermal growth factor receptor (EGFR), a trans-membrane glycoprotein, belongs to a family (erbB) of closely related cell membrane receptors such as EGFR (erbB-1 or HER1), erbB-2 (HER2), erbB-3 (HER3), and erbB-4 (HER4) [8-12]. The dysregulation, expression or over expression of EGFR has been discovered to be associated with numerous human solid tumors such as breast, ovarian, non-small cell lung (NSCLC), colorectal, head and neck [13-17]. EGFR activation can enhance tumor growth by increasing cell proliferation, motility [18], adhesion and invasive capacity [19], and by apoptosis inhibition [20]. The strategy of regulating the signaling of EGFR in the treatment of cancer has been revealed lately by a range of molecular inhibitors which have been developed and are going through clinical trials.

Alternatively, a 125 KD non-receptor protein tyrosine kinase (focal adhesion kinase, FAK), controls cell proliferation, survival and migration in reaction to extracellular signals [21, 22]. The triggering of FAK is initiated by the binding of integrin to extra cellular matrix (ECM), followed by FAK autophosphorylation at Tyr-397, which is vital for majority of cell functions [23]. The FAK phosphorylation is vital in stimulating FAK-dependent transduction of signal as its state of phosphorylation can control the capability of these molecules to interact with

phosphatidylinositol 3-kinase and Src, and/or it controls FAK catalytic activity which impacts these molecules' ability to become phosphorylated [24]. FAK's amino-terminal domain holds an area which shares sequence correspondence to Four-point-one, ezrin, radixin, moesin (FERM) domains, which might be an indication in controlling the phosphorylation state and activity of FAK in cells [25]. Several tumors such as thyroid, brain, liver, prostate, breast, colon, head and neck have been discovered to overexpress FAK. Moreover, this over-expression is associated with an invasive phenotype in such tumors [26-28]. The invasion of ovarian cancer cells and glioblastomas was found to be reduced by FAK signaling inhibition via over-expression of dominant-negative FAK fragments [29]. Additionally, the involvement of FAK in survival, angiogenesis, metastasis and invasion of cancer cell has been also discovered [30]. Therefore, the search for FAK inhibitor offers a new understanding of the anti-tumor ability.

Along with DNA, microtubules are one of the most strategic and logical molecular targets among all the existing ones for chemotherapy. Owing to better biological relevance and understanding of microtubule as a target for cancer therapy, tubulin inhibitors have been under the spotlight as cancer therapeutics for the past few years leading to comprehensive preclinical and clinical studies of several agents. Nonetheless, owing to the failure of numerous agents to exhibit effectiveness in phase III studies, certain novel inhibitors together with formerly studied agents (in various combinations and malignancies) are being clinically evaluated.

The main hindrance in the successful tumor chemotherapy includes the development of resistance in tumor cells against cytotoxic agents and the failure in discovery of novel anticancer agents possessing multi target approach. Due to the structural irrelativeness of this resistance to cytostatics, it was termed multidrug resistance (MDR), which is categorized by a reduced responsiveness to cytotoxic agents. So far, researchers have been struggling to overcome or

circumvent multidrug resistance (MDR) in cancer [31, 32]. Hence, MDR remains one of the main complications for efficacious treatment of tumor. The most discussed mechanism of MDR states that the efflux of chemotherapeutic drugs from cells takes place by 'drug pumps' [33]. Chemotherapeutics which have not been found to be the substrates of drug efflux pumps have gained attention in current drug development approaches to overcome MDR. Furthermore, in clinical trials, efforts to overcome resistance to chemotherapeutics by using MDR modulators for the past 20 years have not yielded promising results [34, 35]. Drugs which efficiently target drug-resistant tumors are the need of the hour. In spite of massive research endeavours and rapid progress made, there is an increasing demand for new therapies as ever. It is vital to find new targets and novel multifunctional agents for cancer treatment.

On the basis of our earlier findings, we have strived to find novel compounds with multiple functions and in doing so we have expanded our previously reported work [36-38] by synthesizing 34 new α , β -unsaturated carbonyl-based compounds. The novelty of this work lies in the incorporation of ligustrazine chemically known as tetramethylpyrazine (TMP) in new compounds as it has been recently reported to be a beneficial adjuvant in the reversal of MDR in tumor cells. For instance, in response to Adr TMP was discovered to improve the chemosensitivity of human hepatocellular carcinoma cells [39]. TMP is a vital component of Chinese conventional medicinal herb chuanxiong (*Ligusticum chuanxiong Hort*). In current study, a series of novel α , β -unsaturated carbonyl-based compounds with TMP moiety was designed, synthesized and assessed for its anticancer potential on human cancer cell lines. Among these, the 6 most active compounds were selected as precursors for additional synthesis to their oxime derivatives. The 12 most potent among all 34 compounds were designated for

anticancer mechanistic studies for their effects on BRAF^{V600E}, EGFR TK kinases, FAK and tubulin polymerization and were tested *in vitro* to reverse MDR developed by cancer cells.

RESULTS AND DISCUSSION

Chemistry

In this study, 34 novel cyclohexanone compounds and a few with cyclohexanone-extended oxime backbone were synthesized as previously reported[38, 40] (Table 1), however tetra methyl pyrazine (TMP) was introduced in synthesis as new modification. Starting from ligustrazine (**1**), 2-hydroxymethyl-3,5,6-trimethylpyrazine (**2**) was first synthesized by Boekelheide reaction. An aldehyde group-containing intermediate (**3**) was produced after 2-iodoxybenzoic acid (IBX) oxidation of (**2**) (Scheme 1). Claisen Schmidt condensation was used between suitable aryl aldehydes including TMP-based aldehyde (**3**) and various cyclohexanone ketone linkers (**4a-g**) at a molar ratio 2:1 for the synthesis of desired α , β -unsaturated carbonyl-based compounds (**5a-g**) and (**6a-u**), (Scheme 1). Of cyclohexanone backbone, all novel compounds contained ligustrazine (TMP)-based aldehyde either on one side (**6a-6u**) or on both sides (**5a-g**). The derivatives of cyclohexanone bearing TMP-based aldehyde on one side contained different aldehyde types with various substitution patterns on the other as previously reported. To synthesize oxime analogs, specific cyclohexanone derivatives were used as precursors. For yielding respective oximes, hydroxylamine hydrochloride was allowed to react with each selected compound. HPLC analysis revealed that all newly synthesized compounds were more than 95% pure. All compounds were subjected to microanalysis (CHNS), HRMS, ¹³C NMR, ¹H NMR and melting point (MP) analyses and their details are provided in experimental part.

Cell viability assay

The rule of three (activity-exposure-toxicity) is the most difficult challenge faced by potential new drugs in the phase of design and development. In drug discovery, absorption, distribution, metabolism and excretion (ADME) studies are frequently performed to convert lead compounds into drugs which are both effective and safe [41]. To perform *in vitro* cell viability assay, human mammary gland epithelial cells (MCF-10A) were used. The MCF-10A cells were exposed to synthesized compounds for 96h and MTT assay was used to investigate cell viability. The results are shown as percentage toxicity (Table 2). All compounds exhibited a cell viability percentage of more than 88% and were found to be safe.

Antiproliferative effects of synthetic compounds

Propidium iodide (PI) fluorescence assay was carried out to assess the compounds' cytotoxicity to the A-549 (epithelial cancer cell line), PC-3 (prostate cancer cell line), MCF-7 (breast cancer cell line), PaCa-2 (pancreatic carcinoma cell line) and HT-29 (colon cancer cell line). Erlotinib hydrochloride (Tarceva), a drug used to treat pancreatic and non-small cell lung cancer (NSCLC) cells is a receptor tyrosine kinase inhibitor which acts on the epidermal growth factor receptor (EGFR) resulting in blocking the signals within the cancer cells and inhibiting EGFR activity followed by cell death. Erlotinib was used as a positive control in this study.

The results of cell viability assays (on different cell lines) of all compounds were almost the same (antiproliferative) and the difference in their inhibitory activities was lesser than 11%. Among all compounds (including erlotinib and precursor α , β -unsaturated carbonyl-based compounds), oximes **7(b,e,f)** and **8(f,o,r)** exhibited best antiproliferative activity with the values of IC_{50} in the range of $0.01 \pm 0.01 \mu\text{M}$ to $0.1 \pm 0.08 \mu\text{M}$ (Table 2). Compound **7e** was found to be

the best antiproliferative agent against all cancer cells. As reported earlier, the compounds were found to be active against only one or two cell lines.

The structural variations can be correlated with the activity of compounds. Owing to the presence of cyclohexanone linkers, oximes were found to be more active than precursor α , β -unsaturated carbonyl-based compounds. Compounds bearing same linker but substituted aldehyde on one side and TMP on the other side of linker were found to be less potent as compared to those containing the dual incorporation of TMP moiety on both sides of linkers. Better tumor growth inhibitory potential of compound **5a** in comparison to compounds **6a-c** could be attributed to the presence of double TMP moiety in **5a**. Similar activity pattern was seen among other compounds with the same linker. Wang et al. previously reported a new derivative of ligustrazine which showed extremely low toxicity and potent antitumor activity by COX-2 and NF- κ B/p65 suppression in S180 mice [42].

Compounds (**5e** and **6o**) bearing were discovered to be most potent in comparison to compounds containing other linkers. After 1-methyl-piperidin-4-one, 1-Isopropyl-piperidin-4-one linker turned out to be most active with 4-methyl-cyclohexanone linker (**5b**, **6d** and **6f**) also showing noteworthy effects on the growth of cancer cells.

The substitution patterns at R_2 , R_3 , and R_4 of second arm aldehydes for synthesizing **6a-u** also showed activity difference. The derivatives of cyclohexanone bearing single methoxy groups at position 3 were discovered to be less active in comparison to those containing two methoxy groups at positions 2 and 3. On the benzene ring of all compounds, halogens (Cl or Br) were present at position 4. As no compound from this sequence of compounds was free from halogen, the halogen influence on compound activity could not be detected. The mechanistic effects of most active antiproliferative compounds on tubulin polymerization, EGFR TK kinases, KAF and

BRAF^{V600E} were investigated, followed by *in vitro* investigation of reversal of efflux-based resistance developed by cancer cells

EGFR inhibitory activity

EGFR might get activated due to mutations, over-expression leading to autocrine expression or constitutive activation of ligand[43, 44]. Ras expression in cells over-expressing EGFR also leads to substantial activation of EGFR-induced apoptosis signifying that activation of Ras is an important survival signal produced by EGFR. So, for developing novel therapies for cancer treatment, EGFR kinase is an attractive target. Apart from other classes of inhibitors, 4-(phenylamino) quinazolines have been discovered to be most potent [45-47].

To evaluate the EGFR inhibitory potential of compounds, EGFR-TK assay was performed (Table 3). The findings of the cancer cell-based assays have been complemented by the results from this assay. All compounds showed potent EGFR inhibition with IC₅₀ in the range of 0.02±0.01 to 4.1±1.0 μM. The compounds **7e** and **8o** displayed comparable and most potent activities (IC₅₀ = 0.02±0.01 μM) among all compounds (including positive control). After **7e** and **8o**, compound **5e** was also found to be more effective than positive control. Similar to erlotinib, 1-methyl-piperidin-4-one-bearing compound **6o** inhibited the activity of EGFR (IC₅₀ = 0.06±0.05 μM). Focusing on the chemical structure, compound **6o** bears an aldehyde on one side of the linker whereas a TMP-based aldehyde lies on the other side with substitutions of methoxy groups at R₂ and R₃ and halogen at R₄ position of aromatic ring. Xu and coworkers reported the synthesis of a similar series of α, β-unsaturated cyclohexanone analogues of curcumin, they investigated their antiproliferative effect using two cancer cell lines and also determined their inhibitory activity against EGFR TK kinases. For both studies the effects of compounds were found to be remarkable[48]. The incorporation of different linkers and TMP moiety improved the

activity of compounds in comparison to the data reported previously. This study shows the compounds to be strong inhibitors of EGFR and can probably be used as anticancer agents.

BRAF^{V600E} inhibitory activity

In the BRAF activation segment, a valine to glutamate substitution at position 600 (V600E) has been discovered to be responsible for 90% of cancer-related mutations of BRAF, and BRAF^{V600E} displays enhanced transformation and increased activity of kinases in melanocytes and fibroblasts *in vitro* [5, 49-52]. A comprehensive cancer genome mutation mapping has revealed BRAF mutation in 7% of human cancers, and this finding signifies BRAF as a key oncogene, predominantly in melanomas. These collective findings render BRAF kinase as a promising target for the development of anticancer drugs.

Ten most active compounds were subjected to *in vitro* BRAF^{V600E} inhibitory assay. All compounds exhibited IC₅₀ ranging from 0.7±0.4-3.1±0.4 μM (Table 3). Compounds possessing TMP moiety on both sides of the linker were found to be strong inhibitors of BRAF^{V600E}. The strongest activity was shown by compound **5e** bearing TMP dual moiety and 1-methyl-piperidin-4-one linker. In comparison to parent cyclohexanone derivatives, oximes were discovered to be less potent. In comparison to compounds bearing TMP core on one side and methoxy-substituted aldehydes on the other, compounds possessing TMP backbone on both sides of linker were found to be more active. The compounds were discovered to be effective inhibitors of BRAF enzyme and can be referred to as prospective anticancer agents. From a library of 23000 compounds, 2-(3,4,5-trimethoxyphenylamino)-6-(3-acetamidophenyl)-pyrazine was discovered to be a potent inhibitor (IC₅₀ 3.5 μM) of BRAF[53]. Lately, a 2,6-disubstituted pyrazine scaffold designated from a high output screening has yielded a new BRAF^{V600E} inhibitor series. Pyrazine inhibitors which were potent (<500 nM) and selective (5-86-fold) against BRAF in comparison

to CRAF were obtained [53]. In comparison to previously reported 2-(3,4,5-Trimethoxyphenylamino)-6-(3-acetamidophenyl)-pyrazine, TMP-containing compounds synthesized in this study were discovered to be more active.

FAK inhibitory assay

Through effects on the stromal cells of the tumor microenvironment and on cancer cells, FAK stimulates metastasis and tumor progression. Cancer stem cell self-renewal, gene expression, survival, invasion and cell movement are regulated by FAK's kinase-dependent and independent functions. Small-molecule inhibitors of FAK have been discovered to decrease metastasis and tumor growth in numerous preclinical models with lesser adverse effects. The FAK inhibitory potency of compounds was investigated and the findings revealed most of the compounds to be active against FAK (Table 3). Comparable to erlotinib (IC_{50} 7.4 ± 1.5 μ M), compound **7f** exhibited the best inhibitory activity (IC_{50} 1.0 ± 0.2 μ M) among all compounds. Best FAK inhibitory effects were exhibited by 1-Isopropyl-piperidin-4-one linker-bearing compounds (**5f**, **6r**, **7f** and **8r**) followed by 1-methyl-piperidin-4-one linker-bearing compounds (**5e**, **6o**, **7e** and **8o**), whereas compounds bearing 4-methyl-cyclohexanone linker (**5b**, **6f**, **7b** and **8f**) were discovered to be least active. In comparison to precursor α , β -unsaturated carbonyl-based compounds (**5f** and **6r**), oximes (**7f** and **8r**) were found to be more active FAK inhibitors.

Effects on tubulin polymerization

Microtubule-targeting agents interfere with microtubule function and stop mitosis, resulting in necrosis and apoptosis and ultimately cell death [54, 55]. The effect of twelve selected synthetic compounds on tubulin polymerization was investigated. Most compounds inhibited the assembly of tubulin with compounds **5b** and **6f** turning out to be most potent inhibitors. On the other hand, compounds (**5e** and **8o**) did not inhibit the assembly of tubulin suggesting a mechanism of action

other than tubulin inhibition for the observed cytotoxicity. In comparison to model drug docetaxel, no compound exhibited promising microtubule-stabilizing action [56]. After analysis, it was observed that 4-methyl-cyclohexanone moiety played key role for the inhibition of tubulin polymerization while 1-methyl-piperidin-4-one core-bearing compounds (**5e**, **6o**, **7e** and **8o**) were found to be potent inhibitors of EGFR; however, they did not show the inhibition of tubulin assembly.

MDR reversal activity

MDR of tumor cells is a main hurdle to the efficacy of chemotherapy [57]. Rhodamine accumulation experiment was carried out to investigate the effect of compounds at nontoxic concentration on the accumulation of drugs in MDR cancer cells (Table 3). Trypan blue experiment was carried out to study the toxic effects of new synthetic compounds. The compounds were nontoxic to cells at 50 $\mu\text{g/mL}$ concentration. On R123 accumulation, most of compounds were ineffective at 5 $\mu\text{g/ml}$ concentration. After an incubation of 30 min, the compounds reversed the MDR on mouse lymphoma cells at a concentration of 50 $\mu\text{g/mL}$. The positive control used in the experiment was verapamil. The cyclohexanone derivatives (**5b**, **e** and **f**) bearing TMP arms on both sides and oximes **7(b, e and f)** were found to be most active. The fluorescence activity ratio (FAR) of 1 or more signified that the compounds were able to reverse MDR. The MDR modulators bind to Pgp trans-membrane domains, bringing about Pgp structural change resulting in the prevention of ABC transporter activity [58]. All compounds were discovered to be active against human *mdr1* gene-transfected cells of mouse lymphoma.

The sensitivity of K562/A02 cells to Adriamycin (Adr) and subsequent cytotoxicity was found to be enhanced using a ligustrazine derivate as it enhanced Adr intracellular accumulation. The

TMP derivative-induced Adr accumulation was linked with down regulation of GSTp expression and GST-associated enzyme activity [59]. MDR of cancer cells can be reversed using a combination of resistance modifiers and traditional chemotherapeutics. Compounds possessing double properties as MDR modulators and as strong anticancer agents can be potential candidates for the treatment of cancer.

Molecular Docking Study

In order to gain some structural insights into both FAK and EGFR inhibitory activities of the newly synthesized compounds, a molecular docking simulation was performed using LIGANDFIT embedded in the Discovery Studio software (Accelrys® software corporation, San Diego, USA). The 3D crystal structure of FAK (PDB IDs: 2JKO) in complex with bis-anilino pyrimidine inhibitor, TAF089, and 3D crystal structure of EGFR (PDB ID: 1M17) in complex with erlotinib were used for this docking study [60, 61]. The most active compounds **5f** and **7f** compared with the least active one **6f** were selected to be docked into the FAK active site where their interactions and binding patterns were investigated. Meanwhile, the active compounds **8o** and **6o** in addition to the least active one **8r** were docked into EGFR binding site using the same docking protocol. The superimposition of the active docked poses inside both proteins binding pockets were presented in **Figure 1**. Initially, the docking protocol settings were validated through the redocking of the extracted co-crystallized ligand TAF089 from the 3D structure 2JKO using the same protocol for compounds **5f**, **6f** and **7f**. Interestingly, the used docking protocol closely reproduced the bound structure with RMSD value of 0.37 Å confirming the confidence in our docking study. The docked pose of TAF089 and the experimental co-crystallized structure have been shown in **Figure 2**.

The inspection of docking results revealed that all the three docked ligands **5f**, **6f** and **7f** adopted a nearly similar disposition inside the ATP binding pocket of the FAK kinase, whereas the common core, piperidinone or cyclohexanone, was leaned between Ile428, Gly429 and Glu506 residues within the kinase hinge region, **Figure 3 (A,B,D)**. Meanwhile, the pyrazine ring bearing three methyl groups made hydrophobic contacts with Gly429, Glu500, Asp564 and Leu567 located near the gatekeeper residue Met499 and DFG motif of FAK activation loop. Obviously, compounds **5f** and **7f** exhibited mostly an identical orientation with a hydrophobic interaction between the isopropyl moiety and Thr503 residue. The slight increase in potency of **7f** ($IC_{50} = 1.0 \mu M$) compared to **5f** ($IC_{50} = 1.2 \mu M$) may be attributed to the additional H-bond interaction formed between the hydroxyl amine moiety in compound **7f** with Ile428 residue in the hinge region of FAK kinase, **Figure 3(C)**. On the contrary, the 2-bromo-4,5-dimethoxybenzylidene moiety in compound **6f** seems to considerably protrude outside the FAK active site owing to its inferior inhibitory activity, **Figure 3(D)**. The superimposition of the two active poses **5f** and **7f** in addition to TAF089 into the active site FAK kinase was shown in **Figure 3**.

On the other hand, the docking results of the most active compound **8o** against EGFR indicated that it fits well inside the ATP-active site forming a network of hydrogen bonds with Lys721, Thr766 and Met769 residues. Also, it was found that the 2-bromo-4,5-dimethoxybenzylidene moiety aligns near the DFG motif which plays a pivotal role in the regulation of kinase activity. The trimethyl pyrazine moiety was oriented towards the hinge region making hydrophobic interactions with Leu694, Gly722 and Phe771 residue. Moreover, the methyl piperidin-4-one core bearing an oxime group was located in the middle of the active site where the oxime was directed towards Met769 and the methyl group directed to the bottom forming a hydrophobic interaction with Leu694 and Val702 residues, **Figure 4(A)**. However, compound **6o** adopted a

similar binding pattern to that of compound **8o**, there was a slight decrease in its EGFR inhibitory activity. The absence of the hydroxyl amine moiety in compound **6o**, which forms an important hydrogen bond with Met769 residue, may greatly contribute to this change in potency, **Figure 4(B)**. Conversely, compound **8r** with the least potency against EGFR adopted a completely reversal orientation and binding pattern compared to compound **8o** where the 2-bromo-4,5-dimethoxybenzylidene moiety was oriented, to some extent, away from the hinge region and the trimethyl pyrazine was located near the DFG motif. Also, the hydroxyl amine moiety was pushed towards the hydrophobic residue Leu694 forming no hydrogen bonds, **Figure 4(C,D)**. This opposite dispositioning may be the reason behind the low potency of compound **8r** against EGFR kinase.

Conclusion

A series of α , β -unsaturated cyclohexanone derivatives bearing different substitutions and ligustrazine incorporation were synthesized and investigated *in vitro* for their antiproliferative effect on 5 different human cancer cell lines. The compounds exhibiting the strongest antiproliferative activities were selected for successive synthesis of oximes and their subsequent assessment through mechanistic studies. New oxime analogs as inhibitors of tubulin polymerization, BRAF^{V600E}, FAK and EGFR-TK have been discovered. MDR reversal activity was exhibited by most of the compounds. In all studies, compounds **5e** and **7e** exhibited potent activities. Hence, we have recognized compounds possessing double properties as MDR modulators and as strong anticancer agents, and have collected some useful SAR evidence which may turn out to be beneficial in the synthesis of additional MDR reversal agents with inherent antitumor activity.

EXPERIMENTAL SECTION

Chemistry General Information:

Acros Organics, Merck and Sigma-Aldrich were the manufacturers whose analytical grade reagents and chemicals were used in this project. ^{13}C and ^1H NMR spectra were recorded on JEOL ECP spectrometer (500 MHz) using CDCl_3 and dimethyl sulfoxide (DMSO-d_6) as solvents while the internal standard used was Me_4Si . High resolution mass spectra (HRMS) were recorded on MicroTOF-Q mass spectrometer (Bruker). Fison EA 1108 elemental analyzer was used to obtain the microanalyses data. Silica gel 60 (230-400 mesh, Merck) was used to carry out flash column chromatography whereas thin layer chromatography (TLC) was performed using pre-coated silica plates (kiesel gel 60 F_{254} , BDH). The melting points of compounds were determined using an electrothermal instrument. After burning on a hotplate, the compounds were examined using vanillin stain or under UV light (254 nm). To determine the purity of compounds, Beckmann system Gold HPLC equipped with Kinetex C18 Coloumn (250mmX mm, $5\mu\text{m}$) was used with a linear gradient from 0% to 100% solvent B (0.1% TFA/ 40% water/ 60% acetonitrile). Compounds **3** and **4** were synthesized as reported previously [62]. All the compounds were discovered to be more than 95% pure.

Synthesis of ligustrazine containing α , β -unsaturated carbonyl based compounds

New α , β -unsaturated carbonyl-based compounds (**5a-g** and **6a-u**) were synthesized using direct coupling technique [40] (Scheme 1). The reaction was carried out using base-catalyzed Claisen-Schmidt condensation reaction, by reacting different types of ketones with appropriate aromatic aldehyde at molar ratio 2:1 to synthesize new compounds (**5a-g**) and at molar ratio 1:1 for (**6a-u**). For synthesis of **6a-u** first **5a-g** intermediates were synthesized and in second step appropriate

aldehydes were reacted with intermediates. The detailed method of synthesis has already been reported by us previously [38, 40]. Scheme 1 shows the highlights of synthesis of compound **3**, **4** and α , β -unsaturated carbonyl-based compounds along with oxime derivatives. 15 mL ethanol was taken in a round bottom flask and aromatic aldehyde (20 mmol, 2 equivalent) and specific ketone (10 mmol, 1 equivalent) were added and dissolved using a stirrer for 2-3 min at 5°C. Into the above solution, 40% NaOH solution in ethanol was added drop wise and the mixture was stirred for 1-24 h at 27°C. The color change and precipitate formation in the reaction mixture showed product formation. TLC was used to monitor the reaction and acidified ice was added to quench the reaction once completed. The isolation of compounds was done by recrystallization and/or by using column chromatography.

2,6-Bis-(3,5,6-trimethyl-pyrazin-2-ylmethylene)-cyclohexanone (5a)

Yield: 74%; Mp: 112-113 °C; ¹H NMR (500 MHz, CDCl₃) δ : 7.87 (s, 2H), 2.55 (s, 6H); 2.51 (s, 6H); 2.48 (s, 6H); 2.37 (t, J=8.0 Hz, 4H), 1.85 (m, 2H); ¹³C NMR (500 MHz, CDCl₃) δ : 181.2, 152.7, 150.4, 149.6, 147.9, 146.2, 141.4, 27.9, 27.1, 17.1, 16.8, 16.1; HRMS (ESI) m/z: 363.4754 [M+H]⁺, Microanalysis calculated for C₂₂H₂₆N₄O (362.47), C: 72.90%, H: 7.23%, N: 15.46%. Found C: 72.96%, H: 7.25%, N: 15.42%.

2,6-bis-(3,5,6-trimethyl-pyrazin-2-ylmethylene)-4-methyl-cyclohexanone (5b)

Yield: 69%; Mp: 108-109 °C; ¹H NMR (500 MHz, CDCl₃) δ : 7.89 (s, 2H), 2.59 (s, 6H); 2.54 (s, 6H); 2.50 (s, 6H); 2.07 (d, J=8.5 Hz, 4H), 1.72 (m, H); 1.19 (d, J=8.5 Hz, 3H); ¹³C NMR (500 MHz, CDCl₃) δ : 180.5, 152.5, 151.1, 149.4, 147.2, 146.1, 140.9, 32.5, 29.2, 22.8, 17.9, 17.0, 16.2; HRMS (ESI) m/z: 377.5029 [M+H]⁺, Microanalysis calculated for C₂₃H₂₈N₄O (376.49), C: 73.37%, H: 7.50%, N: 14.88%. Found C: 73.45%, H: 7.52%, N: 14.67%.

2,6-bis-(3,5,6-trimethyl-pyrazin-2-ylmethylene)- 4-isopropyl-cyclohexanone (5c)

Yield: 61%; Mp: 121-122 °C; ¹H NMR (500 MHz, CDCl₃) δ: 7.92 (s, 2H), 2.55 (s, 12H); 2.51 (s, 6H); 2.09 (d, J=8 Hz, 4H), 1.75(m, H); 1.65(m, H); 1.14 (d, J=7 Hz, 6H); ¹³C NMR (500 MHz, CDCl₃) δ: 182.2, 151.8, 150.2, 149.1, 147.0, 146.4, 140.5, 38.5, 30.9, 29.7, 22.1, 17.2, 16.4, 15.5; HRMS (ESI) m/z: 405.5541 [M+H]⁺, Microanalysis calculated for C₂₅H₃₂N₄O (404.55), C: 74.22%, H: 7.97%, N: 13.85%. Found C: 74.28%, H: 7.82%, N: 13.81%.

3,5-Bis-(3,5,6-trimethyl-pyrazin-2-ylmethylene)-piperidin-4-one (5d)

Yield: 65%; Mp: 147-148 °C; ¹H NMR (500 MHz, CDCl₃) δ: 7.91 (s, 2H), 2.61 (s, 6H); 2.57 (s, 6H); 2.50 (s, 6H); 2.68 (s, 4H); ¹³C NMR (500 MHz, CDCl₃) δ: 182.1, 152.5, 150.6, 149.2, 147.8, 146.1, 142.5, 47.2, 17.8, 17.1, 16.2; HRMS (ESI) m/z: 364.4677 [M+H]⁺, Microanalysis calculated for C₂₁H₂₅N₅O (363.46), C: 69.40%, H: 6.93%, N: 19.27%. Found C: 69.49%, H: 6.98%, N: 19.01%.

3,5-bis-(3,5,6-trimethyl-pyrazin-2-ylmethylene)-1-methyl-piperidin-4-one (5e)

Yield: 55%; Mp: 149-151 °C; ¹H NMR (500 MHz, CDCl₃) δ: 7.88 (s, 2H), 2.72 (s, 4H); 2.59 (s, 6H); 2.54 (s, 6H); 2.50 (s, 6H); 2.14 (s, 3H); ¹³C NMR (500 MHz, CDCl₃) δ: 182.5, 152.2, 151.1, 149.4, 147.2, 146.0, 142.7, 49.5, 32.7, 17.9, 17.0, 16.3; HRMS (ESI) m/z: 378.4019 [M+H]⁺, Microanalysis calculated for C₂₂H₂₇N₅O (377.48), C: 70.00%, H: 7.21%, N: 18.55%. Found C: 70.29%, H: 7.54%, N: 18.46%.

3,5-bis-(3,5,6-trimethyl-pyrazin-2-ylmethylene)- 1-Isopropyl-piperidin-4-one (5f)

Yield: 59%; Mp: 142-143 °C; ¹H NMR (500 MHz, CDCl₃) δ: 7.81 (s, 2H), 2.57 (s, 6H); 2.52 (s, 6H); 2.47 (s, 6H); 2.27 (s, 4H), 1.60(m, H); 1.12 (d, J=7 Hz, 6H); ¹³C NMR (500 MHz, CDCl₃) δ:

184.1, 152.4, 150.6, 148.1, 147.4, 146.2, 142.9, 49.2, 32.8, 22.1, 18.0, 17.2, 16.6; HRMS (ESI) m/z : 406.5432 $[M+H]^+$, Microanalysis calculated for $C_{24}H_{31}N_5O$ (405.54), C: 71.08%, H: 7.70%, N: 17.27%. Found C: 71.12%, H: 7.96%, N: 17.22%.

3,5-Bis-(3,5,6-trimethyl-pyrazin-2-ylmethylene)-tetrahydro-pyran-4-one (5g)

Yield: 69%; Mp: 127-129 °C; 1H NMR (500 MHz, $CDCl_3$) δ : 7.79 (s, 2H), 2.65 (s, 4H), 2.52 (s, 6H); 2.47 (s, 6H); 2.44 (s, 6H); ^{13}C NMR (500 MHz, $CDCl_3$) δ : 182.5, 152.5, 150.4, 149.0, 147.6, 146.4, 142.2, 52.5, 17.9, 17.4, 16.5; HRMS (ESI) m/z : 365.4482 $[M+H]^+$, Microanalysis calculated for $C_{21}H_{24}N_4O_2$ (364.44), C: 69.21%, H: 6.64%, N: 15.37%. Found C: 69.29%, H: 6.68%, N: 15.27%.

2-(2-Chloro-benzylidene)-6-(3,5,6-trimethyl-pyrazin-2-ylmethylene)-cyclohexanone (6a)

Yield: 68%; Mp: 124-125 °C; 1H NMR (500 MHz, $CDCl_3$) δ : 7.91 (s, H), 7.77 (s, H), 7.39 (d, $J=7.0$ Hz, H), 7.19 (d, $J=7.0$ Hz, H), 6.80 (t, $J=7.5$ Hz, H), 6.62 (t, $J=7.5$ Hz, H), 2.61 (s, 9H); 2.39 (t, $J=8.0$ Hz, 4H), 1.87 (m, 2H); ^{13}C NMR (500 MHz, $CDCl_3$) δ : 181.7, 152.4, 150.1, 149.5, 147.2, 146.4, 145.2, 141.7, 135.5, 132.2, 130.4, 128.9, 128.1, 126.5, 27.6, 27.0, 17.9, 16.9, 16.5; HRMS (ESI) m/z : 353.8659 $[M+H]^+$, Microanalysis calculated for $C_{21}H_{21}ClN_2O$ (352.86), C: 71.48%, H: 6.00%, N: 7.94%. Found C: 71.59%, H: 6.28%, N: 7.65%.

2-(2-Chloro-4-methoxy-benzylidene)-6-(3,5,6-trimethyl-pyrazin-2-ylmethylene)-cyclohexanone (6b)

Yield: 72%; Mp: 133-134 °C; 1H NMR (500 MHz, $CDCl_3$) δ : 7.87 (s, H), 7.62 (s, H), 7.35 (d, $J=7.0$ Hz, H), 7.20 (d, $J=7.0$ Hz, H), 6.57 (s, H), 3.51 (s, 3H); 2.67 (s, 6H); 2.61 (s, 3H); 2.35 (t, $J=8.0$ Hz, 4H), 1.82 (m, 2H); ^{13}C NMR (500 MHz, $CDCl_3$) δ : 182.5, 162.2, 157.4, 149.1, 147.5,

146.2, 145.3, 141.5, 134.7, 132.6, 130.8, 126.2, 118.6, 116.9, 55.7, 27.2, 26.4, 15.9, 15.1, 14.2;
HRMS (ESI) m/z : 383.8917 $[M+H]^+$, Microanalysis calculated for $C_{22}H_{23}ClN_2O_2$ (382.88), C:
69.01%, H: 6.05%, N: 7.32%. Found C: 69.15%, H: 6.25%, N: 7.21%.

*2-(2-Bromo-4,5-dimethoxy-benzylidene)-6-(3,5,6-trimethyl-pyrazin-2-ylmethylene)-
cyclohexanone (6c)*

Yield: 74%; Mp: 132-133 °C; 1H NMR (500 MHz, $CDCl_3$) δ : 7.88 (s, H), 7.42 (s, H), 7.15 (s,
H), 6.29 (s, H), 3.59 (s, 6H); 2.61 (s, 3H); 2.54 (s, 3H); 2.49 (s, 3H); 2.36 (t, $J=8.0$ Hz, 4H), 1.89
(m, 2H); ^{13}C NMR (500 MHz, $CDCl_3$) δ : 182.0, 162.8, 156.6, 148.6, 147.2, 146.0, 145.5, 141.2,
135.1, 132.9, 130.2, 126.4, 118.2, 117.1, 55.7, 55.0, 27.9, 26.5, 15.6, 15.0, 14.4; HRMS (ESI)
 m/z : 458.3671 $[M+H]^+$, Microanalysis calculated for $C_{23}H_{25}BrN_2O_3$ (457.36), C: 60.40%, H:
5.51%, N: 6.13%. Found C: 60.49%, H: 5.89%, N: 6.01%.

*2-(2-Chloro-benzylidene)-4-methyl-6-(3,5,6-trimethyl-pyrazin-2-ylmethylene)-cyclohexanone
(6d)*

Yield: 68%; Mp: 141-142 °C; 1H NMR (500 MHz, $CDCl_3$) δ : 7.99 (s, H), 7.76 (s, H), 7.32 (d,
 $J=7.0$ Hz, H), 7.14 (d, $J=7.0$ Hz, H), 6.87 (t, $J=7.0$ Hz, H), 6.60 (t, $J=7.0$ Hz, H), 2.62 (s, 6H);
2.57 (s, 3H); 2.05 (d, $J=8.5$ Hz, 4H), 1.70 (m, H); 1.14 (d, $J=8.5$ Hz, 3H); ^{13}C NMR (500 MHz,
 $CDCl_3$) δ : 181.2, 152.7, 150.8, 149.1, 147.6, 146.2, 145.3, 141.2, 135.6, 132.4, 130.9, 128.6,
127.4, 126.2, 32.2, 29.5, 22.6, 17.3, 16.9, 16.0; HRMS (ESI) m/z : 367.8925 $[M+H]^+$,
Microanalysis calculated for $C_{22}H_{23}ClN_2O$ (366.88), C: 72.02%, H: 6.32%, N: 7.64%. Found C:
72.25%, H: 6.57%, N: 7.58%.

*2-(2-Chloro-4-methoxy-benzylidene)-4-methyl-6-(3,5,6-trimethyl-pyrazin-2-ylmethylene)-
cyclohexanone (6e)*

Yield: 62%; Mp: 129-130 °C; ¹H NMR (500 MHz, CDCl₃) δ: 7.97 (s, H), 7.68 (s, H), 7.41 (d, J=7.0 Hz, H), 7.24 (d, J=7.0 Hz, H), 6.52 (s, H), 3.54(s, 3H); 2.64 (s, 3H); 2.54 (s, 3H); 2.49 (s, 3H); 2.10 (d, J=8.5 Hz, 4H), 1.79 (m, H); 1.21 (d, J=8.5 Hz, 3H); ¹³C NMR (500 MHz, CDCl₃) δ: 181.6, 159.6, 152.2, 149.4, 148.1, 146.7, 145.2, 141.5, 135.4, 132.2, 130.6, 128.1, 127.2, 126.3, 57.5, 32.9, 28.1, 22.4, 18.1, 17.2, 16.5; HRMS (ESI) m/z: 397.9172 [M+H]⁺, Microanalysis calculated for C₂₃H₂₅ClN₂O₂ (396.91), C: 69.60%, H: 6.35%, N: 7.06%. Found C: 69.90%, H: 6.52%, N: 6.89%.

2-(2-Bromo-4,5-dimethoxy-benzylidene)-4-methyl-6-(3,5,6-trimethyl-pyrazin-2-ylmethylene)-cyclohexanone (6f)

Yield: 71%; Mp: 147-148 °C; ¹H NMR (500 MHz, CDCl₃) δ: 7.92 (s, H), 7.59 (s, H), 7.07 (s, H), 6.27 (s, H), 3.64(s, 6H); 2.60 (s, 3H); 2.55 (s, 3H); 2.49 (s, 3H); 2.12 (d, J=8.5 Hz, 4H), 1.76 (m, H); 1.14 (d, J=8.5 Hz, 3H); ¹³C NMR (500 MHz, CDCl₃) δ: 182.1, 160.2, 152.8, 150.7, 148.6, 146.3, 145.1, 141.2, 136.3, 132.7, 130.8, 128.6, 127.0, 126.2, 57.7, 56.9, 32.4, 28.6, 21.9, 18.7, 17.9, 17.2; HRMS (ESI) m/z: 472.3952 [M+H]⁺, Microanalysis calculated for C₂₄H₂₇BrN₂O₃ (471.39), C: 61.15%, H: 5.77%, N: 5.94%. Found C: 61.29%, H: 5.90%, N: 5.82%.

2-(2-Chloro-benzylidene)-4-isopropyl-6-(3,5,6-trimethyl-pyrazin-2-ylmethylene)-cyclohexanone (6g)

Yield: 59%; Mp: 119-120 °C; ¹H NMR (500 MHz, CDCl₃) δ: 7.90 (s, H), 7.66 (s, H), 7.24 (d, J=7.0 Hz, H), 7.04 (d, J=7.0 Hz, H), 6.81 (t, J=7.0 Hz, H), 6.59 (t, J=7.0 Hz, H), 2.57 (s, 9H); 2.07 (d, J=8 Hz, 4H), 1.88(m, H); 1.71(m, H); 1.11(d, J=7 Hz, 6H); ¹³C NMR (500 MHz, CDCl₃) δ: 184.6, 152.8, 150.6, 149.8, 147.4, 146.1, 145.0, 140.2, 135.9, 131.1, 130.2, 128.3, 127.4, 126.1, 38.2, 30.6, 29.2, 22.5, 18.4, 17.8, 16.5; HRMS (ESI) m/z: 395.9451 [M+H]⁺,

Microanalysis calculated for C₂₄H₂₇ClN₂O (394.94), C: 72.99%, H: 6.89%, N: 7.09%. Found C: 73.21%, H: 6.99%, N: 7.02%.

2-(2-Chloro-4-methoxy-benzylidene)-4-isopropyl-6-(3,5,6-trimethyl-pyrazin-2-ylmethylene)-cyclohexanone (6h)

Yield: 57%; Mp: 113-114 °C; ¹H NMR (500 MHz, CDCl₃) δ: 7.94 (s, H), 7.70 (s, H), 7.37 (d, J=7.0 Hz, H), 7.14 (d, J=7.0 Hz, H), 6.50 (s, H), 3.59(s, 3H); 2.59 (s, 9H); 2.05 (d, J=8 Hz, 4H), 1.80 (m, H); 1.72 (m, H); 1.10 (d, J=7 Hz, 6H); ¹³C NMR (500 MHz, CDCl₃) δ: 182.9, 159.3, 152.4, 149.2, 147.3, 146.5, 144.9, 140.5, 134.8, 132.6, 130.1, 128.7, 126.9, 125.2, 58.2, 39.5, 32.8, 28.7, 22.9, 17.9, 17.1, 16.3; HRMS (ESI) m/z: 425.9705 [M+H]⁺, Microanalysis calculated for C₂₅H₂₉ClN₂O₂ (424.96), C: 70.66%, H: 6.88%, N: 6.59%. Found C: 70.72%, H: 6.93%, N: 6.27%.

2-(2-Bromo-4,5-dimethoxy-benzylidene)-4-isopropyl-6-(3,5,6-trimethyl-pyrazin-2-ylmethylene)-cyclohexanone (6i)

Yield: 67%; Mp: 128-129 °C; ¹H NMR (500 MHz, CDCl₃) δ: 7.91 (s, H), 7.64 (s, H), 7.05 (s, H), 6.22 (s, H), 3.61(s, 6H); 2.52 (s, 9H); 2.06 (d, J=8 Hz, 4H), 1.77(m, H); 1.69 (m, H); 1.12 (d, J=7 Hz, 6H); ¹³C NMR (500 MHz, CDCl₃) δ: 182.5, 158.6, 153.5, 148.7, 147.1, 146.4, 143.2, 140.1, 133.5, 132.2, 130.5, 128.9, 127.2, 125.1, 58.9, 57.4, 39.6, 32.3, 28.4, 23.1, 17.8, 17.4, 16.8; HRMS (ESI) m/z: 500.4480 [M+H]⁺, Microanalysis calculated for C₂₆H₃₁BrN₂O₃ (499.44), C: 62.53%, H: 6.26%, N: 5.61%. Found C: 62.79%, H: 6.29%, N: 5.55%.

3-(2-Chloro-benzylidene)-5-(3,5,6-trimethyl-pyrazin-2-ylmethylene)-piperidin-4-one (6j)

Yield: 62%; Mp: 121-121 °C; ¹H NMR (500 MHz, CDCl₃) δ: 7.90 (s, H), 7.70 (s, H), 7.31 (d, J=7.0 Hz, H), 7.12 (d, J=7.0 Hz, H), 6.85 (t, J=7.0 Hz, H), 6.64 (t, J=7.0 Hz, H), 2.92 (s, 4H); 2.60 (s, 3H); 2.55 (s, 3H); 2.50 (s, 3H); ¹³C NMR (500 MHz, CDCl₃) δ: 182.1, 152.5, 150.6, 149.2, 147.8, 146.1, 144.9, 142.5, 135.9, 131.1, 130.2, 128.3, 127.4, 126.1, 44.6, 18.1, 17.9, 16.8; HRMS (ESI) m/z: 354.8535 [M+H]⁺, Microanalysis calculated for C₂₀H₂₀ClN₃O (353.84), C: 67.89%, H: 5.70%, N: 11.88%. Found C: 67.91%, H: 5.72%, N: 11.85%.

3-(2-Chloro-4-methoxy-benzylidene)-5-(3,5,6-trimethyl-pyrazin-2-ylmethylene)-piperidin-4-one (6k)

Yield: 75%; Mp: 141-142 °C; ¹H NMR (500 MHz, CDCl₃) δ: 7.89 (s, H), 7.67 (s, H), 7.29 (d, J=7.0 Hz, H), 7.15 (d, J=7.0 Hz, H), 6.48 (s, H), 3.56 (s, 3H); 2.97 (s, 4H); 2.59 (s, 3H); 2.54 (s, 3H); 2.49 (s, 3H); ¹³C NMR (500 MHz, CDCl₃) δ: 182.4, 160.7, 154.4, 148.5, 147.3, 146.7, 144.5, 141.3, 134.6, 131.4, 130.6, 128.7, 127.8, 126.4, 57.7, 48.3, 18.2, 17.5, 16.8; HRMS (ESI) m/z: 384.8797 [M+H]⁺, Microanalysis calculated for C₂₁H₂₂ClN₃O₂ (383.87), C: 65.71%, H: 5.78%, N: 10.95%. Found C: 65.92%, H: 5.79%, N: 10.82%.

3-(2-Bromo-4,5-dimethoxy-benzylidene)-5-(3,5,6-trimethyl-pyrazin-2-ylmethylene)-piperidin-4-one (6l)

Yield: 79%; Mp: 139-140 °C; ¹H NMR (500 MHz, CDCl₃) δ: 7.85 (s, H), 7.62 (s, H), 7.07 (s, H), 6.25 (s, H), 3.62 (s, 6H); 2.95 (s, 4H); 2.52 (s, 3H); 2.47 (s, 3H); 2.41 (s, 3H); ¹³C NMR (500 MHz, CDCl₃) δ: 183.5, 160.1, 155.2, 148.1, 147.2, 146.5, 144.6, 141.5, 133.9, 131.6, 130.0, 128.8, 127.4, 126.5, 58.2, 57.3, 48.7, 18.6, 17.8, 17.0; HRMS (ESI) m/z: 459.3572 [M+H]⁺,

Microanalysis calculated for $C_{22}H_{24}BrN_3O_3$ (458.34), C: 57.65%, H: 5.28%, N: 9.17%. Found C: 57.69%, H: 5.35%, N: 9.05%.

3-(2-Chloro-benzylidene)-1-methyl-5-(3,5,6-trimethyl-pyrazin-2-ylmethylene)-piperidin-4-one
(6m)

Yield: 84%; Mp: 119-120 °C; 1H NMR (500 MHz, $CDCl_3$) δ : 7.86 (s, H), 7.61 (s, H), 7.27 (d, $J=7.0$ Hz, H), 7.10 (d, $J=7.0$ Hz, H), 6.87 (t, $J=7.0$ Hz, H), 6.61 (t, $J=7.0$ Hz, H), 2.70 (s, 4H); 2.59 (s, 3H); 2.52 (s, 3H); 2.49 (s, 3H); 2.15 (s, 3H); ^{13}C NMR (500 MHz, $CDCl_3$) δ : 184.1, 152.4, 150.3, 149.2, 147.1, 146.2, 145.3, 142.5, 136.2, 132.4, 130.5, 128.2, 127.1, 126.7, 48.4, 32.5, 17.6, 17.1, 16.5; HRMS (ESI) m/z : 368.8795 $[M+H]^+$, Microanalysis calculated for $C_{21}H_{22}ClN_3O$ (367.87), C: 68.56%, H: 6.03%, N: 11.42%. Found C: 68.61%, H: 6.11%, N: 11.22%.

3-(2-Chloro-4-methoxy-benzylidene)-1-methyl-5-(3,5,6-trimethyl-pyrazin-2-ylmethylene)-piperidin-4-one **(6n)**

Yield: 79%; Mp: 117-118 °C; 1H NMR (500 MHz, $CDCl_3$) δ : 7.88 (s, H), 7.67 (s, H), 7.26 (d, $J=7.0$ Hz, H), 7.14 (d, $J=7.0$ Hz, H), 6.43 (s, H), 3.55 (s, 3H); 2.78 (s, 4H); 2.57 (s, 3H); 2.51 (s, 3H); 2.49 (s, 3H); 2.17 (s, 3H); ^{13}C NMR (500 MHz, $CDCl_3$) δ : 182.9, 162.1, 156.2, 149.5, 147.6, 146.0, 145.2, 142.2, 135.6, 132.5, 129.8, 128.5, 127.4, 126.2, 58.3, 49.2, 32.7, 17.9, 17.0, 16.4; HRMS (ESI) m/z : 398.9055 $[M+H]^+$, Microanalysis calculated for $C_{22}H_{24}ClN_3O_2$ (397.89), C: 66.41%, H: 6.08%, N: 10.56%. Found C: 66.57%, H: 6.29%, N: 10.29%.

3-(2-Bromo-4,5-dimethoxy-benzylidene)-1-methyl-5-(3,5,6-trimethyl-pyrazin-2-ylmethylene)-piperidin-4-one (6o)

Yield: 74%; Mp: 134-135 °C; ¹H NMR (500 MHz, CDCl₃) δ: 7.84 (s, H), 7.67 (s, H), 7.09 (s, H), 6.21 (s, H), 3.65(s, 6H); 2.75 (s, 4H); 2.59 (s, 3H); 2.55 (s, 3H); 2.50 (s, 3H); 2.14 (s, 3H); ¹³C NMR (500 MHz, CDCl₃) δ: 182.6, 161.9, 156.5, 150.2, 147.3, 146.1, 145.7, 141.6, 135.2, 131.8, 129.2, 128.7, 127.2, 126.4, 58.9, 57.6, 50.0, 32.6, 17.4, 16.9, 16.3; HRMS (ESI) m/z: 473.3825 [M+H]⁺, Microanalysis calculated for C₂₃H₂₆BrN₃O₃ (472.37), C: 58.48%, H: 5.55%, N: 8.90%. Found C: 58.52%, H: 5.67%, N: 8.87%.

3-(2-Chloro-benzylidene)-1-isopropyl-5-(3,5,6-trimethyl-pyrazin-2-ylmethylene)-piperidin-4-one (6p)

Yield: 79%; Mp: 128-129 °C; ¹H NMR (500 MHz, CDCl₃) δ: 7.91 (s, H), 7.65 (s, H), 7.26 (d, J=7.0 Hz, H), 7.14 (d, J=7.0 Hz, H), 6.80 (t, J=7.0 Hz, H), 6.57 (t, J=7.0 Hz, H), 2.69 (s, 3H); 2.64 (s, 3H); 2.57 (s, 3H); 2.24 (s, 4H), 1.61(m, H); 1.09 (d, J=7 Hz, 6H); ¹³C NMR (500 MHz, CDCl₃) δ: 185.0, 154.6, 150.2, 148.7, 147.6, 146.4, 144.0, 142.8, 136.7, 132.3, 130.0, 128.7, 127.6, 126.4, 48.4, 31.6, 23.4, 18.7, 17.9, 17.0; HRMS (ESI) m/z: 396.9329 [M+H]⁺, Microanalysis calculated for C₂₃H₂₆ClN₃O (395.92), C: 69.77%, H: 6.62%, N: 10.61%. Found C: 69.79%, H: 6.69%, N: 10.55%.

3-(2-Chloro-4-methoxy-benzylidene)-1-isopropyl-5-(3,5,6-trimethyl-pyrazin-2-ylmethylene)-piperidin-4-one (6q)

Yield: 61%; Mp: 132-133 °C; ¹H NMR (500 MHz, CDCl₃) δ: 7.92 (s, H), 7.63 (s, H), 7.22 (d, J=7.0 Hz, H), 7.19 (d, J=7.0 Hz, H), 6.41 (s, H), 3.58 (s, 3H); 2.62 (s, 3H); 2.58 (s, 3H); 2.54 (s, 3H); 2.27 (s, 4H), 1.52(m, H); 1.07 (d, J=7 Hz, 6H); ¹³C NMR (500 MHz, CDCl₃) δ: 184.8,

160.2, 154.1, 148.5, 147.9, 146.3, 144.2, 141.4, 135.4, 131.9, 130.2, 129.1, 128.1, 127.4, 59.2, 49.9, 32.8, 24.6, 18.1, 17.5, 16.9; HRMS (ESI) m/z : 426.9592 $[M+H]^+$, Microanalysis calculated for $C_{24}H_{28}ClN_3O_2$ (425.95), C: 67.67%, H: 6.63%, N: 9.87%. Found C: 67.72%, H: 6.65%, N: 9.82%.

3-(2-Bromo-4,5-dimethoxy-benzylidene)-1-isopropyl-5-(3,5,6-trimethyl-pyrazin-2-ylmethylene)-piperidin-4-one (6r)

Yield: 62%; Mp: 126-127 °C; 1H NMR (500 MHz, $CDCl_3$) δ : 7.97 (s, H), 7.71 (s, H), 7.10 (s, H), 6.27 (s, H), 3.69 (s, 6H); 2.60 (s, 3H); 2.53 (s, 3H); 2.49 (s, 3H); 2.26 (s, 4H), 1.50(m, H); 1.05 (d, $J=7$ Hz, 6H); ^{13}C NMR (500 MHz, $CDCl_3$) δ : 184.0, 160.4, 154.5, 148.7, 147.6, 146.2, 143.8, 141.8, 134.2, 131.8, 130.7, 129.4, 128.6, 127.2, 58.7, 58.0, 48.4, 32.9, 24.5, 18.6, 17.8, 17.0; HRMS (ESI) m/z : 501.4355 $[M+H]^+$, Microanalysis calculated for $C_{25}H_{30}BrN_3O_3$ (500.42), C: 60.00%, H: 6.04%, N: 8.40%. Found C: 60.22%, H: 6.15%, N: 8.41%.

3-(2-Chloro-benzylidene)-5-(3,5,6-trimethyl-pyrazin-2-ylmethylene)-tetrahydro-pyran-4-one (6s)

Yield: 54%; Mp: 112-113 °C; 1H NMR (500 MHz, $CDCl_3$) δ : 7.78 (s, H), 7.63 (s, H), 7.22 (d, $J=7.0$ Hz, H), 7.09 (d, $J=7.0$ Hz, H), 6.73 (t, $J=7.0$ Hz, H), 6.55 (t, $J=7.0$ Hz, H), 2.61 (s, 4H), 2.50 (s, 3H); 2.47 (s, 3H); 2.43 (s, 3H); ^{13}C NMR (500 MHz, $CDCl_3$) δ : 182.6, 152.4, 150.7, 149.8, 148.1, 147.2, 146.1, 141.9, 134.6, 131.7, 131.0, 129.8, 128.2, 127.3, 54.7, 17.7, 17.0, 16.6; HRMS (ESI) m/z : 355.8385 $[M+H]^+$, Microanalysis calculated for $C_{20}H_{19}ClN_2O_2$ (354.83), C: 67.70%, H: 5.40%, N: 7.89%. Found C: 67.84%, H: 5.45%, N: 7.95%.

3-(2-Chloro-4-methoxy-benzylidene)-5-(3,5,6-trimethyl-pyrazin-2-ylmethylene)-tetrahydro-pyran-4-one (6t)

Yield: 58%; Mp: 119-120 °C; ¹H NMR (500 MHz, CDCl₃) δ: 7.86 (s, H), 7.69 (s, H), 7.27 (d, J=7.0 Hz, H), 7.04 (d, J=7.0 Hz, H), 6.52 (s, H), 3.61 (s, 3H); 2.72 (s, 4H), 2.56 (s, 3H); 2.52 (s, 3H); 2.48 (s, 3H); ¹³C NMR (500 MHz, CDCl₃) δ: 182.9, 159.6, 154.2, 149.7, 148.4, 147.2, 146.7, 141.5, 133.9, 131.2, 130.2, 129.3, 128.4, 127.5, 58.8, 54.3, 17.9, 17.2, 16.5; HRMS (ESI) m/z: 385.8640 [M+H]⁺, Microanalysis calculated for C₂₁H₂₁ClN₂O₃ (384.85), C: 65.54%, H: 5.50%, N: 7.28%. Found C: 65.59%, H: 5.72%, N: 7.15%.

3-(2-Bromo-4,5-dimethoxy-benzylidene)-5-(3,5,6-trimethyl-pyrazin-2-ylmethylene)-tetrahydro-pyran-4-one (6u)

Yield: 59%; Mp: 121-122 °C; ¹H NMR (500 MHz, CDCl₃) δ: 7.89 (s, H), 7.67 (s, H), 7.12 (s, H), 6.24 (s, H), 3.69 (s, 6H); 2.78 (s, 4H), 2.55 (s, 3H); 2.51 (s, 3H); 2.48 (s, 3H); ¹³C NMR (500 MHz, CDCl₃) δ: 182.3, 159.8, 153.6, 148.9, 148.0, 147.1, 146.4, 142.2, 132.7, 131.6, 130.9, 129.0, 128.5, 127.3, 58.2, 57.7, 54.2, 17.5, 17.0, 16.6; HRMS (ESI) m/z: 460.3412 [M+H]⁺, Microanalysis calculated for C₂₂H₂₃BrN₂O₄ (459.33), C: 57.53%, H: 5.05%, N: 6.10%. Found C: 57.58%, H: 5.12%, N: 6.05%.

Synthesis of oxime analogs

Most potent inhibitors of cancer cells growth from ligustrazine containing α , β -unsaturated carbonyl based compounds were selected as precursors for the synthesis of oxime analogs. For oxime synthesis, hydroxylamine hydrochloride (2 mmol) was reacted with each selected compound (1 mmol) in 10 mL ethanol to yield the respective oxime (**7b**, **7e**, **7f**, **8f**, **8o** and **8r**). The average completion time of a reaction was around 6-8 h, as determined by TLC.

The purity of the product was determined by using TLC. The product was recrystallized from ethyl acetate to yield solid powder. Column chromatography using ethyl acetate: hexane (70:30 v/v) as eluent was used to purify certain products.

4-Methyl-2,6-bis-(3,5,6-trimethyl-pyrazin-2-ylmethylene)-cyclohexanone oxime (7b)

Yield: 49%; Mp: 110-111 °C; ¹H NMR (500 MHz, CDCl₃) δ: 8.40 (s, H), 7.45 (s, 2H), 2.57 (s, 6H); 2.52 (s, 6H); 2.49 (s, 6H); 2.05 (d, J=8.5 Hz, 4H), 1.70 (m, H); 1.12 (d, J=8.5 Hz, 3H); ¹³C NMR (500 MHz, CDCl₃) δ: 168.5, 153.6, 152.1, 149.2, 147.0, 145.4, 140.6, 32.7, 29.1, 21.8, 17.7, 17.1, 16.6; HRMS (ESI) m/z: 392.5172 [M+H]⁺, Microanalysis calculated for C₂₃H₂₉N₅O (391.50), C: 70.56%, H: 7.47%, N: 17.89%. Found C: 70.77%, H: 7.49%, N: 17.59%.

3,5-bis-(3,5,6-trimethyl-pyrazin-2-ylmethylene)-1-methyl-piperidin-4-one oxime (7e)

Yield: 55%; Mp: 152-153 °C; ¹H NMR (500 MHz, CDCl₃) δ: 8.37 (s, H), 7.48 (s, 2H), 2.70 (s, 4H); 2.57 (s, 6H); 2.53 (s, 6H); 2.49 (s, 6H); 2.12 (s, 3H); ¹³C NMR (500 MHz, CDCl₃) δ: 166.4, 154.1, 151.3, 149.4, 147.1, 146.7, 142.2, 49.2, 32.1, 17.8, 17.1, 16.5; HRMS (ESI) m/z: 393.5055 [M+H]⁺, Microanalysis calculated for C₂₂H₂₈N₆O (392.49), C:67.15%, H: 7.43%, N: 21.36%. Found C: 67.29%, H: 7.47%, N: 21.20%.

3,5-bis-(3,5,6-trimethyl-pyrazin-2-ylmethylene)-1-Isopropyl-piperidin-4-one oxime (7f)

Yield: 44%; Mp: 151-152 °C; ¹H NMR (500 MHz, CDCl₃) δ: 8.39 (s, H), 7.41 (s, 2H), 2.55 (s, 6H); 2.52 (s, 6H); 2.48 (s, 6H); 2.22 (s, 4H), 1.56 (m, H); 1.09 (d, J=7 Hz, 6H); ¹³C NMR (500 MHz, CDCl₃) δ: 164.7, 152.1, 150.2, 148.4, 147.2, 146.1, 142.4, 49.7, 32.3, 22.5, 18.1, 17.7, 16.8; HRMS (ESI) m/z: 421.5584 [M+H]⁺, Microanalysis calculated for C₂₄H₃₂N₆O (420.55), C: 68.54%, H: 7.67%, N: 19.98%. Found C: 68.55%, H: 7.76%, N: 19.75%.

2-(2-Bromo-4,5-dimethoxy-benzylidene)-4-methyl-6-(3,5,6-trimethyl-pyrazin-2-ylmethylene)-cyclohexanone oxime (8f)

Yield: 58%; Mp: 154-155 °C; ¹H NMR (500 MHz, CDCl₃) δ: 8.41 (s, H), 7.52 (s, H), 7.39 (s, H), 6.90 (s, H), 6.12 (s, H), 3.62 (s, 6H); 2.59 (s, 3H); 2.54 (s, 3H); 2.50 (s, 3H); 2.06 (d, J=8.5 Hz, 4H), 1.69 (m, H); 1.03 (d, J=8.5 Hz, 3H); ¹³C NMR (500 MHz, CDCl₃) δ: 162.4, 158.1, 152.3, 150.2, 148.4, 146.5, 145.7, 141.5, 135.2, 132.4, 130.3, 128.7, 127.2, 126.5, 57.9, 57.0, 32.5, 28.7, 21.2, 18.5, 17.8, 17.0; HRMS (ESI) m/z: 487.4095 [M+H]⁺, Microanalysis calculated for C₂₄H₂₈BrN₃O₃ (486.40), C: 59.14%, H: 6.00%, N: 8.62%. Found C: 59.27%, H: 6.14%, N: 8.74%.

3-(2-Bromo-4,5-dimethoxy-benzylidene)-1-methyl-5-(3,5,6-trimethyl-pyrazin-2-ylmethylene)-piperidin-4-one oxime (8o)

Yield: 72%; Mp: 141-142 °C; ¹H NMR (500 MHz, CDCl₃) δ: 8.36 (s, H), 7.62 (s, H), 7.34 (s, H), 6.87 (s, H), 6.12 (s, H), 3.60 (s, 6H); 2.72 (s, 4H); 2.58 (s, 3H); 2.55 (s, 3H); 2.51 (s, 3H); 2.10 (s, 3H); ¹³C NMR (500 MHz, CDCl₃) δ: 165.9, 157.4, 152.3, 150.5, 147.5, 145.5, 144.1, 141.5, 135.7, 132.2, 129.1, 128.4, 127.3, 126.2, 58.6, 57.7, 50.4, 32.7, 17.8, 16.6, 16.1; HRMS (ESI) m/z: 488.3982 [M+H]⁺, Microanalysis calculated for C₂₃H₂₇BrN₄O₃ (487.38), C: 56.68%, H: 5.58%, N: 11.50%. Found C: 56.78%, H: 5.72%, N: 11.47%.

3-(2-Bromo-4,5-dimethoxy-benzylidene)-1-isopropyl-5-(3,5,6-trimethyl-pyrazin-2-ylmethylene)-piperidin-4-one oxime (8r)

Yield: 54%; Mp: 129-130 °C; ¹H NMR (500 MHz, CDCl₃) δ: 8.41 (s, H), 7.64 (s, H), 7.40 (s, H), 6.97 (s, H), 6.06 (s, H), 3.64 (s, 6H); 2.59 (s, 3H); 2.54 (s, 3H); 2.50 (s, 3H); 2.21 (s, 4H), 1.52 (m, H); 1.08 (d, J=7 Hz, 6H); ¹³C NMR (500 MHz, CDCl₃) δ: 165.6, 160.2, 154.3, 147.7, 146.1,

145.7, 143.2, 141.4, 135.2, 131.6, 130.2, 129.9, 128.1, 127.6, 58.5, 57.9, 48.2, 32.4, 24.9, 18.8, 17.9, 17.2; HRMS (ESI) m/z : 516.4506 $[M+H]^+$, Microanalysis calculated for $C_{25}H_{31}BrN_4O_3$ (515.44), C: 58.25%, H: 6.06%, N: 10.87%. Found C: 58.52%, H: 6.25%, N: 10.56%.

MTT assay

MTT assay was carried out to study the effect of compounds on mammary epithelial cells (MCF-10A) [36]. The medium in which cells were propagated contained Dulbecco's modified Eagle's medium (DMEM)/ Ham's F-12 medium (1:1) supplemented with epidermal growth factor (20 ng/mL), hydrocortisone (500 ng/mL), insulin (10 μ g/mL), 2 mM glutamine and 10% fetal calf serum. After every 2-3 days, the cells were passaged using trypsin ethylenediamine tetra acetic acid (EDTA). The cells were seeded at a density of 10^4 cells mL^{-1} in flat-bottomed culture plates containing 96 wells each. After 24 h, medium was removed from the plates and the compounds in (in 0.1% DMSO) were added (in 200 μ L medium to yield a final concentration of 0.1% v/v) to the wells of plates. A single compound was designated with four wells followed by incubation of plates for 96h at 37°C. After incubation, medium was removed completely from the plates followed by addition of MTT (0.4 mg/mL in medium) to each well and subsequent incubation of plates for 3h. MTT (along with the medium) was removed and DMSO (150 μ L) was added to each well of the culture plates, followed by vortexing and subsequent measurement of absorbance (at 540 nm) using microplate reader. The data are shown as percentage inhibition of proliferation in comparison with controls containing 0.1% DMSO.

Assay for antiproliferative effect

To explore the antiproliferative potential of compounds propidium iodide fluorescence assay[36] was performed using different cell lines such as A-549 (epithelial cancer cell line), PC-3 (prostate cancer cell line), MCF-7 (breast cancer cell line), PaCa-2 (pancreatic carcinoma cell

line), HT-29 (colon cancer cell line) respectively. To calculate the total nuclear DNA, a fluorescent dye (propidium iodide, PI) is used which can attach to the DNA, thus offering a quick and precise technique. PI cannot pass through the cell membrane and its signal intensity can be considered as directly proportional to quantity of cellular DNA. Cells whose cell membranes are damaged or have changed permeability are counted as dead ones. The assay was performed by seeding the cells of different cell lines at a density of 3000-7500 cells/well (in 200µl medium) in culture plates followed by incubation for 24h at 37 °C in humidified 5% CO₂/95% air atmospheric conditions. The medium was removed; the compounds were added to the plates at 10 µM concentrations (in 0.1% DMSO) in triplicates, followed by incubation for 48 h. DMSO (0.1%) was used as control. After incubation, medium was removed followed by the addition of PI (25 µl, 50µg/mL in water/medium) to each well of the plates. At -80 °C, the plates were allowed to freeze for 24 h, followed by thawing at 25°C. A fluorometer (Polar-Star BMG Tech) was used to record the readings at excitation and emission wavelengths of 530 and 620 nm for each well. The percentage cytotoxicity of compounds was calculated using the following formula:

$$\% \text{ Cytotoxicity} = \frac{A_c - A_{TC}}{A_c} \times 100$$

Where A_{TC} = Absorbance of treated cells and A_c = Absorbance of control. Erlotinib was used as positive control in the assay.

EGFR inhibitory assay

Baculoviral expression vectors including pBlueBacHis2B and pFASTBacHTc were used separately to clone 1.6 kb cDNA coding for EGFR cytoplasmic domain (EGFR-CD, amino acids 645–1186). 5' upstream to the EGFR sequence comprised a sequence that encoded (His)₆. Sf-9

cells were infected for 72h for protein expression. The pellets of Sf-9 cells were solubilized in a buffer containing sodium vanadate (100 μ M), aprotinin (10 μ g/mL), triton (1%), HEPES buffer (50mM), ammonium molybdate (10 μ M), benzamidine HCl (16 μ g/mL), NaCl (10 mM), leupeptin (10 μ g/mL) and pepstatin (10 μ g/mL) at 0°C for 20 min at pH 7.4, followed by centrifugation for 20 min. To eliminate the nonspecifically bound material, a Ni-NTA superflow packed column was used to pass through and wash the crude extract supernatant first with 10 mM and then with 100 mM imidazole. Histidine-linked proteins were first eluted with 250 and then with 500 mM imidazole subsequent to dialysis against NaCl (50 mM), HEPES (20 mM), glycerol (10%) and 1 μ g/mL each of aprotinin, leupeptin and pepstatin for 120 min. The purification was performed either at 4 °C or on ice. To record autophosphorylation level, EGFR kinase assay was carried out on the basis of DELFIA/Time-Resolved Fluorometry. The compounds were first dissolved in DMSO absolute, subsequent to dilution to appropriate concentration using HEPES (25 mM) at pH 7.4. Each compound (10 μ L) was incubated with recombinant enzyme (10 μ L, 5 ng for EGFR, 1:80 dilution in 100 mM HEPES) for 10 min at 25°C, subsequent to the addition of 5X buffer (10 μ L, containing 2 mM $MnCl_2$, 100 μ M Na_3VO_4 , 20 mM HEPES and 1 mM DTT) and ATP- $MgCl_2$ (20 μ L, containing 0.1 mM ATP and 50 mM $MgCl_2$) and incubation for 1h. The negative and positive controls were included in each plate by the incubation of enzyme either with or without ATP- $MgCl_2$. The liquid was removed after incubation and the plates were washed thrice using wash buffer. Europium-tagged antiphosphotyrosine antibody (75 μ L, 400 ng) was added to each well followed by incubation of 1h and then washing of the plates using buffer. The enhancement solution was added to each well and the signal was recorded at excitation and emission wavelengths of 340 at 615 nm. The

autophosphorylation percentage inhibition by compounds was calculated using the following equation:

$$100\% - [(negative\ control)/(positive\ control) - (negative\ control)]$$

Using the curves of percentage inhibition of eight concentrations of each compound, IC₅₀ was calculated. Majority of signals detected by antiphosphotyrosine antibody were from EGFR because the enzyme preparation contained low impurities.

BRAF kinase assay

V600E mutant BRAF kinase assay was performed to investigate the activity of each compound. Mouse full-length GST-tagged BRAF^{V600E} (7.5 ng, Invitrogen, PV3849) was pre-incubated with drug (1 μL) and assay dilution buffer (4 μL) for 60 min at 25°C. In assay dilution buffer, a solution (5 μL) containing MgCl₂ (30 mM), ATP (200 μM), recombinant human full length (200 ng) and *N*-terminal His-tagged MEK1 (Invitrogen) was added to start the assay, subsequent to incubation for 25 min at 25°C. The assay was stopped using 5X protein denaturing buffer (LDS) solution (5 μL). To further denature the protein, heat (70° C) was applied for 5 min. 4-12% precast NuPage gel plates (Invitrogen) were used to carry out electrophoresis (at 200 V). 10 μL of each reaction was loaded into the precast plates and electrophoresis was allowed to proceed. After completion of electrophoresis, the front part of the precast gel plate (holding hot ATP) was cut and afterwards cast-off. The dried gel was developed using a phosphor screen. A reaction without active enzyme was used as negative control while that containing no inhibitor served as positive control. To study the effect of compounds on cell-based pERK1/2 activity in cancer cells, commercially available ELISA kits (Invitrogen) were used according to manufacturer's instructions.

FAK inhibitory assay

FAK (10 μM) was pre-incubated with different concentrations of compounds in glutamate buffer to study the effect of compounds on FAK assembly *in vitro* at 30°C and subsequently cooled to 0 °C. GTP was added to the reaction mix followed by transferring it to 0 °C cuvettes in a spectrophotometer and warming up to 30°C. The FAK assembly was studied turbid metrically. The concentration of compound which inhibited 50% assembly of FAK after 20 min incubation was termed as IC₅₀ [63].

Tubulin polymerization assay

A commercially available tubulin Polymerization Assay Kit (Cytoskeleton Inc., Denver, CO, USA) which works on the principle of fluorescent reporter enhancement[64] was used to investigate the activity of compounds on tubulin polymerization. FLUO star OPTIMA was used to record (in triplicates) the fluorescence of compounds dissolved in DMSO (5 and 25 μM). Vincristine (3 μM in PBS) and docetaxel (3 μM in PBS) were used as positive destabilizing and stabilizing controls [37].

MDR-reversal assay

For MDR-reversal assay [38], L5178 mouse T-cell lymphoma cells (ATCC, USA) were transfected with PHa MDR1/A retrovirus. Colchicine (60 ng/mL) was cultured with *mdr1*-expressing cell line to maintain MDR expression. The medium used to culture human *mdr1*-transfected subline and L5178 (parental) mouse T-cell lymphoma cell line was McCoy's 5A (supplemented with L-glutamine, 10% heat-inactivated horse serum and antibiotics), with temperature maintained at 37°C and CO₂ level maintained at 5%. The cells were re-suspended in serum-less McCoy's 5A medium at 2×10^6 /mL density, followed by transfer of 0.5 mL aliquots to eppendorf tubes. At different concentrations (4 and 40 $\mu\text{g}/\text{mL}$), the compounds were added to

tubes subsequent to incubation for 10 min at 25°C. After incubation, rhodamine 123 (10 µL, 5.2 µM) was added to the mixture followed by re-incubation for 20 min at 37°C, washing (twice) and re-suspension in PBS (0.5 mL). Flow cytometer was used to record the fluorescence of cell population. Verapamil was used as positive control in rhodamine 123 exclusion assay. In comparison with untreated cells, the fluorescence intensity (%) was recorded for treated and parental MDR cell lines. The activity ratio (R) was calculated on the basis of recorded fluorescence readings, using the following equation:

$$R = \frac{\text{MDR treated/MDR control}}{\text{parental treated/parental control}}$$

Experimental Docking Protocol

The docking simulation was carried out using LIGANDFIT protocol embedded in the Discovery Studio software (Accelrys® software corporation, San Diego, USA). The 3D structures of FAK and EGFR with PDB codes (2JKO and 1M17), respectively were downloaded from Protein Data Bank. The proteins were prepared, cleaned and the hydrogens were added then, the binding sites were generated as volumes of selected co-crystallized ligand. Also, all bound water molecules were eliminated from the protein. The structures of docked compounds were constructed and energetically minimized with CHARMM Force Field using ligand minimization tool and then they were docked according the following protocol; (i) Deriding was employed as the Force Field for calculating ligand-receptor interaction energies with a non-bonded cutoff distance of 10.0 Å and extension of the energy grid from the binding-site of 3.0 Å. The dielectric constant was set to 1.0 to compute the energy grid. (ii) The number of Monte Carlo search trials was fixed at 30000 where search step for torsions with polar hydrogens was equal to 30°. (iii) The

maximum internal energy of 10000 was employed where the ligand conformations with an internal energy higher than this specified value were not docked. (iv) The maximum number of poses retained for each docked compound was 10 poses ranked according to the DOCK-SCORE.

Statistical analysis

All studies were carried out in triplicates and data are presented as mean \pm standard error of mean (SEM). Graph Pad Prism 5 software was used to calculate the IC₅₀ values.

Acknowledgements

HQ and SNAB are grateful to Wuhan University of Technology for financial support.

Notes

“No author has Competing Financial Interest”

REFERENCES

- [1] A. Jemal, R. Siegel, E. Ward, T. Murray, J. Xu, M.J. Thun, *Cancer Statistics*, 2007, CA: A Cancer Journal for Clinicians, 57 (2007) 43-66.
- [2] P. Anand, A.B. Kunnumakkara, C. Sundaram, K.B. Harikumar, S.T. Tharakan, O.S. Lai, B. Sung, B.B. Aggarwal, Cancer is a preventable disease that requires major lifestyle changes, *Pharmaceutical research*, 25 (2008) 2097-2116.
- [3] H.P. Ammon, M.A. Wahl, *Pharmacology of Curcuma longa, Planta medica*, 57 (1991) 1-7.
- [4] S. Dietrich, H. Glimm, M. Andrulis, C. von Kalle, A.D. Ho, T. Zenz BRAF Inhibition in Refractory Hairy-Cell Leukemia, *New England Journal of Medicine*, 366 (2012) 2038-2040.
- [5] H. Davies, G.R. Bignell, C. Cox, P. Stephens, S. Edkins, S. Clegg, J. Teague, H. Woffendin, M.J. Garnett, W. Bottomley, N. Davis, E. Dicks, R. Ewing, Y. Floyd, K. Gray, S. Hall, R. Hawes, J. Hughes, V. Kosmidou, A. Menzies, C. Mould, A. Parker, C. Stevens, S. Watt, S. Hooper, R. Wilson, H. Jayatilake, B.A. Gusterson, C. Cooper, J. Shipley, D. Hargrave, K. Pritchard-Jones, N. Maitland, G. Chenevix-Trench, G.J. Riggins, D.D. Bigner, G. Palmieri, A. Cossu, A. Flanagan, A. Nicholson, J.W.C. Ho, S.Y. Leung, S.T. Yuen, B.L. Weber, H.F. Seigler, T.L. Darrow, H. Paterson, R. Marais, C.J. Marshall, R. Wooster, M.R. Stratton, P.A. Futreal, Mutations of the BRAF gene in human cancer, *Nature*, 417 (2002) 949-954.
- [6] R.B. Corcoran, H. Ebi, A.B. Turke, E.M. Coffee, M. Nishino, A.P. Cogdill, R.D. Brown, P. Della Pelle, D. Dias-Santagata, K.E. Hung, K.T. Flaherty, A. Piris, J.A. Wargo, J. Settleman, M. Mino-Kenudson, J.A. Engelman, EGFR-Mediated Reactivation of MAPK Signaling Contributes to Insensitivity of BRAF-Mutant Colorectal Cancers to RAF Inhibition with Vemurafenib, *Cancer Discovery*, 2 (2012) 227-235.

- [7] G. Bollag, J. Tsai, J. Zhang, C. Zhang, P. Ibrahim, K. Nolop, P. Hirth, Vemurafenib: the first drug approved for BRAF-mutant cancer, *Nat Rev Drug Discov*, 11 (2012) 873-886.
- [8] S. Garofalo, R. Rosa, R. Bianco, G. Tortora, EGFR-targeting agents in oncology, *Expert Opinion on Therapeutic Patents*, 18 (2008) 889-901.
- [9] A. Arora, E.M. Scholar, Role of Tyrosine Kinase Inhibitors in Cancer Therapy, *Journal of Pharmacology and Experimental Therapeutics*, 315 (2005) 971-979.
- [10] Y. Yarden, M.X. Sliwkowski, Untangling the ErbB signalling network, *Nat Rev Mol Cell Biol*, 2 (2001) 127-137.
- [11] G.S. Cockerill, K.E. Lackey, Small molecule inhibitors of the class 1 receptor tyrosine kinase family, *Current topics in medicinal chemistry*, 2 (2002) 1001-1010.
- [12] W. Han, H.-W. Lo, Landscape of EGFR signaling network in human cancers: Biology and therapeutic response in relation to receptor subcellular locations, *Cancer Letters*, 318 (2012) 124-134.
- [13] F. Barlési, C. Tchouhadjian, C. Doddoli, P. Villani, L. Greillier, J.-P. Kleisbauer, P. Thomas, P. Astoul, Gefitinib (ZD1839, Iressa®) in non-small-cell lung cancer: a review of clinical trials from a daily practice perspective, *Fundamental & Clinical Pharmacology*, 19 (2005) 385-393.
- [14] C.L. Arteaga, D.H. Johnson, Tyrosine kinase inhibitors—ZD1839 (Iressa), *Current Opinion in Oncology*, 13 (2001) 491-498.
- [15] A.J. Barker, K.H. Gibson, W. Grundy, A.A. Godfrey, J.J. Barlow, M.P. Healy, J.R. Woodburn, S.E. Ashton, B.J. Curry, L. Scarlett, L. Henthorn, L. Richards, Studies leading to the identification of ZD1839 (iressa™): an orally active, selective epidermal growth factor receptor

tyrosine kinase inhibitor targeted to the treatment of cancer, *Bioorganic & Medicinal Chemistry Letters*, 11 (2001) 1911-1914.

[16] K.N. Ganjoo, H. Wakelee, Review of erlotinib in the treatment of advanced non-small cell lung cancer, *Biologics : Targets & Therapy*, 1 (2007) 335-346.

[17] L. Kopper, Lapatinib: A Sword With Two Edges, *Pathology & Oncology Research*, 14 (2008) 1-8.

[18] Z. Lu, G. Jiang, P. Blume-Jensen, T. Hunter, Epidermal growth factor-induced tumor cell invasion and metastasis initiated by dephosphorylation and downregulation of focal adhesion kinase, *Molecular and cellular biology*, 21 (2001) 4016-4031.

[19] M. Cáceres, J. Guerrero, J. Martínez, Overexpression of RhoA-GTP induces activation of the Epidermal Growth Factor Receptor, dephosphorylation of focal adhesion kinase and increased motility in breast cancer cells, *Experimental Cell Research*, 309 (2005) 229-238.

[20] S. Sengupta, S.L. Smitha, N.E. Thomas, T.R. Santhoshkumar, S.K. Devi, K.G. Sreejalekshmi, K.N. Rajasekharan, 4-Amino-5-benzoyl-2-(4-methoxyphenylamino)thiazole (DAT1): a cytotoxic agent towards cancer cells and a probe for tubulin-microtubule system, *British journal of pharmacology*, 145 (2005) 1076-1083.

[21] D.C. Fingar, J. Blenis, Target of rapamycin (TOR): an integrator of nutrient and growth factor signals and coordinator of cell growth and cell cycle progression, *Oncogene*, 23 (2004) 3151-3171.

[22] V. Thiyagarajan, M.-J. Tsai, C.-F. Weng, Antroquinonol Targets FAK-Signaling Pathway Suppressed Cell Migration, Invasion, and Tumor Growth of C6 Glioma, *PLOS ONE*, 10 (2015) e0141285.

- [23] B.L. Eide, C.W. Turck, J.A. Escobedo, Identification of Tyr-397 as the primary site of tyrosine phosphorylation and pp60src association in the focal adhesion kinase, pp125FAK, *Molecular and cellular biology*, 15 (1995) 2819-2827.
- [24] Z. Xing, H.C. Chen, J.K. Nowlen, S.J. Taylor, D. Shalloway, J.L. Guan, Direct interaction of v-Src with the focal adhesion kinase mediated by the Src SH2 domain, *Molecular biology of the cell*, 5 (1994) 413-421.
- [25] L.A. Cohen, J.-L. Guan, Residues within the First Subdomain of the FERM-like Domain in Focal Adhesion Kinase Are Important in Its Regulation, *Journal of Biological Chemistry*, 280 (2005) 8197-8207.
- [26] A.K. Sood, J.E. Coffin, G.B. Schneider, M.S. Fletcher, B.R. DeYoung, L.M. Gruman, D.M. Gershenson, M.D. Schaller, M.J.C. Hendrix, Biological Significance of Focal Adhesion Kinase in Ovarian Cancer, *The American Journal of Pathology*, 165 1087-1095.
- [27] W.G. Cance, J.E. Harris, M.V. Iacocca, E. Roche, X. Yang, J. Chang, S. Simkins, L. Xu, Immunohistochemical analyses of focal adhesion kinase expression in benign and malignant human breast and colon tissues: correlation with preinvasive and invasive phenotypes, *Clinical cancer research : an official journal of the American Association for Cancer Research*, 6 (2000) 2417-2423.
- [28] V. Thiyagarajan, S.-H. Lin, Y.-C. Chia, C.-F. Weng, A novel inhibitor, 16-hydroxy-cleroda-3,13-dien-16,15-olide, blocks the autophosphorylation site of focal adhesion kinase (Y397) by molecular docking, *Biochimica et Biophysica Acta (BBA) - General Subjects*, 1830 (2013) 4091-4101.
- [29] G. Jones, J. Machado, M. Tolnay, A. Merlo, PTEN-independent Induction of Caspase-mediated Cell Death and Reduced Invasion by the Focal Adhesion Targeting Domain (FAT) in

Human Astrocytic Brain Tumors Which Highly Express Focal Adhesion Kinase (FAK), *Cancer Research*, 61 (2001) 5688-5691.

[30] V.M. Golubovskaya, W.G. Cance, Focal Adhesion Kinase and p53 Signaling in Cancer Cells, in: *International Review of Cytology*, Academic Press, 2007, pp. 103-153.

[31] G.D. Leonard, T. Fojo, S.E. Bates, The role of ABC transporters in clinical practice, *The oncologist*, 8 (2003) 411-424.

[32] C.F. Higgins, Multiple molecular mechanisms for multidrug resistance transporters, *Nature*, 446 (2007) 749-757.

[33] D.W. Shen, C. Cardarelli, J. Hwang, M. Cornwell, N. Richert, S. Ishii, I. Pastan, M.M. Gottesman, Multiple drug-resistant human KB carcinoma cells independently selected for high-level resistance to colchicine, adriamycin, or vinblastine show changes in expression of specific proteins, *The Journal of biological chemistry*, 261 (1986) 7762-7770.

[34] N. Akhtar, A. Ahad, R.K. Khar, M. Jaggi, M. Aqil, Z. Iqbal, F.J. Ahmad, S. Talegaonkar, The emerging role of P-glycoprotein inhibitors in drug delivery: a patent review, *Expert Opinion on Therapeutic Patents*, 21 (2011) 561-576.

[35] A. Saneja, V. Khare, N. Alam, R.D. Dubey, P.N. Gupta, Advances in P-glycoprotein-based approaches for delivering anticancer drugs: pharmacokinetic perspective and clinical relevance, *Expert opinion on drug delivery*, 11 (2014) 121-138.

[36] S.N. Bukhari, I. Jantan, O. Unsal Tan, M. Sher, M. Naeem-Ul-Hassan, H.L. Qin, Biological activity and molecular docking studies of curcumin-related alpha,beta-unsaturated carbonyl-based synthetic compounds as anticancer agents and mushroom tyrosinase inhibitors, *Journal of agricultural and food chemistry*, 62 (2014) 5538-5547.

- [37] H.-L. Qin, Z.-P. Shang, I. Jantan, O.U. Tan, M.A. Hussain, M. Sher, S.N.A. Bukhari, Molecular docking studies and biological evaluation of chalcone based pyrazolines as tyrosinase inhibitors and potential anticancer agents, *RSC Advances*, 5 (2015) 46330-46338.
- [38] H.-L. Qin, J. Leng, C.-P. Zhang, I. Jantan, M.W. Amjad, M. Sher, M. Naeem-ul-Hassan, M.A. Hussain, S.N.A. Bukhari, Synthesis of α,β -Unsaturated Carbonyl-Based Compounds, Oxime and Oxime Ether Analogs as Potential Anticancer Agents for Overcoming Cancer Multidrug Resistance by Modulation of Efflux Pumps in Tumor Cells, *Journal of Medicinal Chemistry*, 59 (2016) 3549-3561.
- [39] X.B. Wang, S.S. Wang, Q.F. Zhang, M. Liu, H.L. Li, Y. Liu, J.N. Wang, F. Zheng, L.Y. Guo, J.Z. Xiang, Inhibition of tetramethylpyrazine on P-gp, MRP2, MRP3 and MRP5 in multidrug resistant human hepatocellular carcinoma cells, *Oncology reports*, 23 (2010) 211-215.
- [40] S.N.A. Bukhari, I. Jantan, V.H. Masand, D.T. Mahajan, M. Sher, M. Naeem-ul-Hassan, M.W. Amjad, Synthesis of α, β -unsaturated carbonyl based compounds as acetylcholinesterase and butyrylcholinesterase inhibitors: Characterization, molecular modeling, QSAR studies and effect against amyloid β -induced cytotoxicity, *European Journal of Medicinal Chemistry*, 83 (2014) 355-365.
- [41] A.-E.F. Nassar, A.M. Kamel, C. Clarimont, Improving the decision-making process in structural modification of drug candidates: reducing toxicity, *Drug Discovery Today*, 9 (2004) 1055-1064.
- [42] C. Zhang, W. Yan, B. Li, B. Xu, Y. Gong, F. Chu, Y. Zhang, Q. Yao, P. Wang, H. Lei, A New Ligustrazine Derivative-Selective Cytotoxicity by Suppression of NF- κ B/p65 and COX-2 Expression on Human Hepatoma Cells. Part 3, *International Journal of Molecular Sciences*, 16 (2015) 16401-16413.

- [43] D.J. Slamon, G.M. Clark, S.G. Wong, W.J. Levin, A. Ullrich, W.L. McGuire, Human breast cancer: correlation of relapse and survival with amplification of the HER-2/neu oncogene, *Science* (New York, N.Y.), 235 (1987) 177-182.
- [44] D.J. Slamon, W. Godolphin, L.A. Jones, J.A. Holt, S.G. Wong, D.E. Keith, W.J. Levin, S.G. Stuart, J. Udove, A. Ullrich, et al., Studies of the HER-2/neu proto-oncogene in human breast and ovarian cancer, *Science* (New York, N.Y.), 244 (1989) 707-712.
- [45] D.W. Fry, A.J. Kraker, A. McMichael, L.A. Ambroso, J.M. Nelson, W.R. Leopold, R.W. Connors, A.J. Bridges, A specific inhibitor of the epidermal growth factor receptor tyrosine kinase, *Science* (New York, N.Y.), 265 (1994) 1093-1095.
- [46] W.H. Ward, P.N. Cook, A.M. Slater, D.H. Davies, G.A. Holdgate, L.R. Green, Epidermal growth factor receptor tyrosine kinase. Investigation of catalytic mechanism, structure-based searching and discovery of a potent inhibitor, *Biochemical pharmacology*, 48 (1994) 659-666.
- [47] A.J. Bridges, H. Zhou, D.R. Cody, G.W. Rewcastle, A. McMichael, H.D. Showalter, D.W. Fry, A.J. Kraker, W.A. Denny, Tyrosine kinase inhibitors. 8. An unusually steep structure-activity relationship for analogues of 4-(3-bromoanilino)-6,7-dimethoxyquinazoline (PD 153035), a potent inhibitor of the epidermal growth factor receptor, *J Med Chem*, 39 (1996) 267-276.
- [48] Y.-Y. Xu, Y. Cao, H. Ma, H.-Q. Li, G.-Z. Ao, Design, synthesis and molecular docking of α,β -unsaturated cyclohexanone analogous of curcumin as potent EGFR inhibitors with antiproliferative activity, *Bioorganic & Medicinal Chemistry*, 21 (2013) 388-394.
- [49] T. Ikenoue, Y. Hikiba, F. Kanai, Y. Tanaka, J. Imamura, T. Imamura, M. Ohta, H. Ijichi, K. Tateishi, T. Kawakami, J. Aragaki, M. Matsumura, T. Kawabe, M. Omata, Functional analysis of

mutations within the kinase activation segment of B-Raf in human colorectal tumors, *Cancer Res*, 63 (2003) 8132-8137.

[50] P.T.C. Wan, M.J. Garnett, S.M. Roe, S. Lee, D. Niculescu-Duvaz, V.M. Good, C.G. Project, C.M. Jones, C.J. Marshall, C.J. Springer, D. Barford, R. Marais, Mechanism of Activation of the RAF-ERK Signaling Pathway by Oncogenic Mutations of B-RAF, *Cell*, 116 855-867.

[51] K. Satyamoorthy, G. Li, M.R. Gerrero, M.S. Brose, P. Volpe, B.L. Weber, P. Van Belle, D.E. Elder, M. Herlyn, Constitutive mitogen-activated protein kinase activation in melanoma is mediated by both BRAF mutations and autocrine growth factor stimulation, *Cancer Res*, 63 (2003) 756-759.

[52] C. Wellbrock, L. Ogilvie, D. Hedley, M. Karasarides, J. Martin, D. Niculescu-Duvaz, C.J. Springer, R. Marais, V599EB-RAF is an oncogene in melanocytes, *Cancer Res*, 64 (2004) 2338-2342.

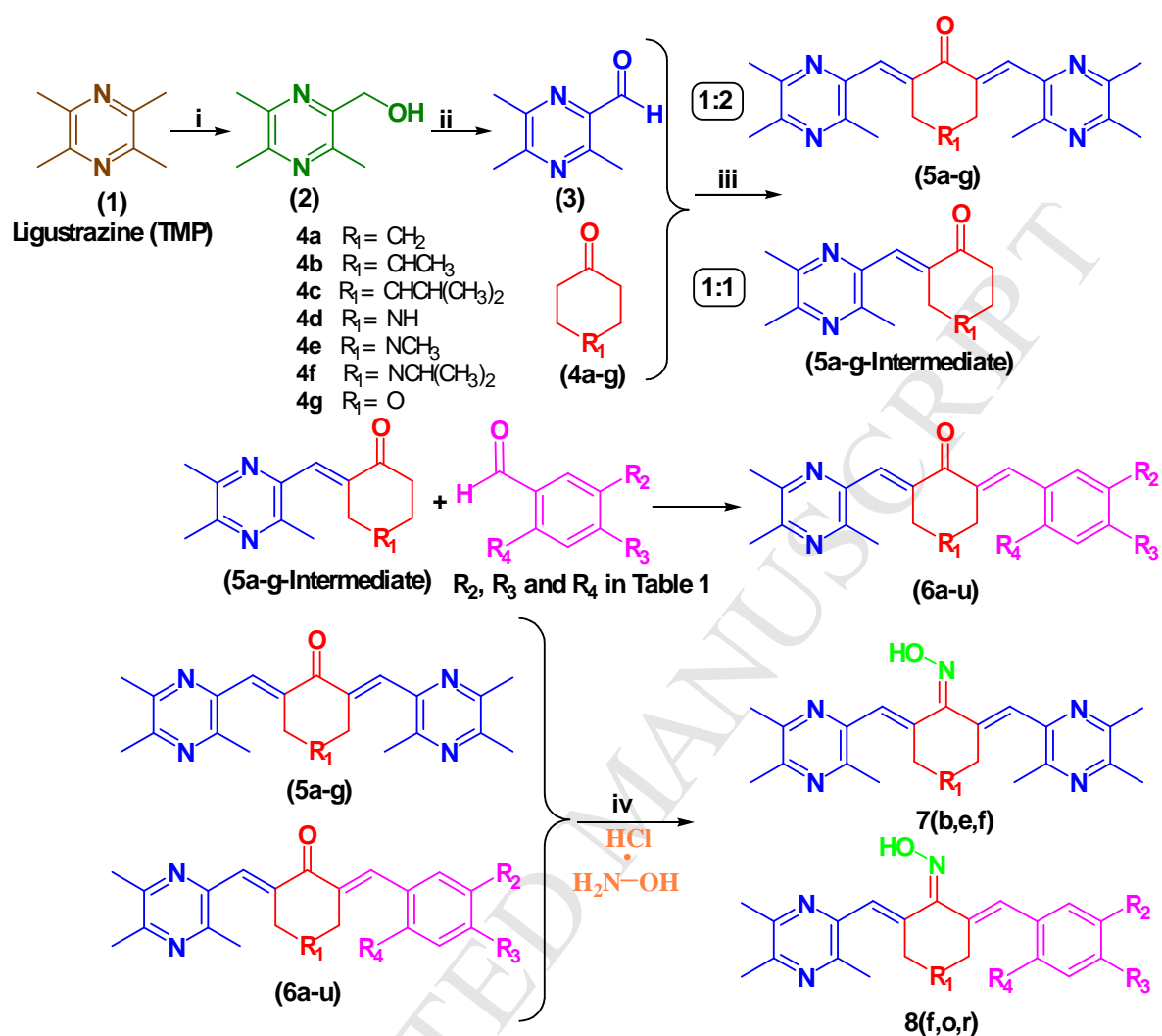
[53] I. Niculescu-Duvaz, E. Roman, S.R. Whittaker, F. Friedlos, R. Kirk, I.J. Scanlon, L.C. Davies, D. Niculescu-Duvaz, R. Marais, C.J. Springer, Novel Inhibitors of the v-raf Murine Sarcoma Viral Oncogene Homologue B1 (BRAF) Based on a 2,6-Disubstituted Pyrazine Scaffold, *Journal of Medicinal Chemistry*, 51 (2008) 3261-3274.

[54] Y. Lu, J. Chen, M. Xiao, W. Li, D.D. Miller, An overview of tubulin inhibitors that interact with the colchicine binding site, *Pharmaceutical research*, 29 (2012) 2943-2971.

[55] A. Jordan, J.A. Hadfield, N.J. Lawrence, A.T. McGown, Tubulin as a target for anticancer drugs: agents which interact with the mitotic spindle, *Medicinal research reviews*, 18 (1998) 259-296.

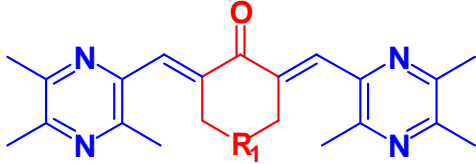
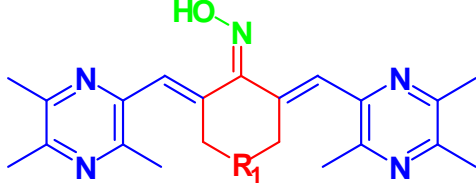
[56] V.A. de Weger, J.H. Beijnen, J.H. Schellens, Cellular and clinical pharmacology of the taxanes docetaxel and paclitaxel--a review, *Anti-cancer drugs*, 25 (2014) 488-494.

- [57] M.M. Gottesman, T. Fojo, S.E. Bates, Multidrug resistance in cancer: role of ATP-dependent transporters, *Nature reviews. Cancer*, 2 (2002) 48-58.
- [58] J. Molnar, N. Gyemant, M. Tanaka, J. Hohmann, E. Bergmann-Leitner, P. Molnar, J. Deli, R. Didiziapetris, M.J. Ferreira, Inhibition of multidrug resistance of cancer cells by natural diterpenes, triterpenes and carotenoids, *Current pharmaceutical design*, 12 (2006) 287-311.
- [59] Ligustrazine derivate DLJ14 reduces multidrug resistance of K562/A02 cells by modulating GST π activity, *Toxicology in Vitro*, (2011).
- [60] D. Lietha, M.J. Eck, Crystal Structures of the FAK Kinase in Complex with TAE226 and Related Bis-Anilino Pyrimidine Inhibitors Reveal a Helical DFG Conformation, *PLOS ONE*, 3 (2008) e3800.
- [61] J. Stamos, M.X. Sliwkowski, C. Eigenbrot, Structure of the epidermal growth factor receptor kinase domain alone and in complex with a 4-anilinoquinazoline inhibitor, *The Journal of biological chemistry*, 277 (2002) 46265-46272.
- [62] X.-C. Cheng, X.-Y. Liu, W.-F. Xu, X.-L. Guo, Y. Ou, Design, synthesis, and biological activities of novel Ligustrazine derivatives, *Bioorganic & Medicinal Chemistry*, 15 (2007) 3315-3320.
- [63] E. Hamel, Evaluation of antimitotic agents by quantitative comparisons of their effects on the polymerization of purified tubulin, *Cell Biochemistry and Biophysics*, 38 (2003) 1-21.
- [64] D. Bonne, C. Heusele, C. Simon, D. Pantaloni, 4',6-Diamidino-2-phenylindole, a fluorescent probe for tubulin and microtubules, *The Journal of biological chemistry*, 260 (1985) 2819-2825.



Scheme 1: Synthesis scheme of α , β -unsaturated carbonyl based compounds, oxime and oxime ether analogs. Reagents and conditions: (i-a) 30% H_2O_2 , acetic acid, 70 $^\circ\text{C}$, 8 h.; (i-b) acetic anhydride, reflux, 2 h; (i-c) 20% NaOH ; (ii) IBX , DMSO , room temperature, 0.5 h; (iii) NaOH , EtOH , Room temperature (iv) $\text{NH}_2\text{OH}\cdot\text{HCl}$, pyridine, ethanol, anhyd., reflux.

Table 1: Structures of new synthetic α , β -unsaturated carbonyl based compounds with ligustrazine moiety.

					
		(4a-g)	7(b,e,f)		
No.	Comp.	R_1			
1.	5a	CH ₂			
2.	5b/7b	CH-CH ₃			
3.	5c	CHCH(CH ₃) ₂			
4.	5d	NH			
5.	5e/7e	N-CH ₃			
6.	5f/7f	NCH(CH ₃) ₂			
7.	5g	O			

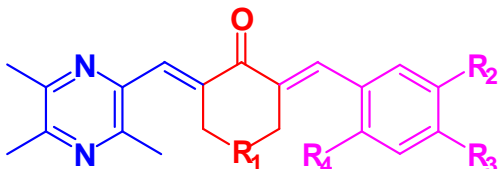
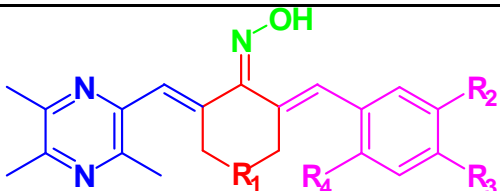
					
		R_1	R_2	R_3	R_4
8.	6a	CH ₂	H	H	Cl
9.	6b	CH ₂	H	OCH ₃	Cl
10.	6c	CH ₂	OCH ₃	OCH ₃	Br
11.	6d	CH-CH ₃	H	H	Cl
12.	6e	CH-CH ₃	H	OCH ₃	Cl
13.	6f/8f	CH-CH ₃	OCH ₃	OCH ₃	Br
14.	6g	CHCH(CH ₃) ₂	H	H	Cl
15.	6h	CHCH(CH ₃) ₂	H	OCH ₃	Cl
16.	6i	CHCH(CH ₃) ₂	OCH ₃	OCH ₃	Br
17.	6j	NH	H	H	Cl
18.	6k	NH	H	OCH ₃	Cl
19.	6l	NH	OCH ₃	OCH ₃	Br
20.	6m	N-CH ₃	H	H	Cl
21.	6n	N-CH ₃	H	OCH ₃	Cl
22.	6o/8o	N-CH ₃	OCH ₃	OCH ₃	Br
23.	6p	NCH(CH ₃) ₂	H	H	Cl
24.	6q	NCH(CH ₃) ₂	H	OCH ₃	Cl
25.	6r/8r	NCH(CH ₃) ₂	OCH ₃	OCH ₃	Br
26.	6s	O	H	H	Cl
27.	6t	O	H	OCH ₃	Cl
28.	6u	O	OCH ₃	OCH ₃	Br

Table 2: Inhibitory effects of synthetic compounds on the growth of normal (MCF-10A) mammary epithelial cells (cell viability) and different types of human cancer cells.

Comp.	Cell viability %	Antiproliferative activity IC ₅₀ ± SEM (µM)				
		A-549	PC-3	MCF-7	PaCa-2	HT-29
5a	91	2.1±0.8	2.4±1.5	2.7±0.6	2.5±0.9	2.2±0.7
5b	97	1.1±1.2	1.0±0.5	1.5±1.0	1.3±0.2	1.7±1.2
5c	93	6.3±0.8	5.7±1.2	6.4±2.2	6.6±2.3	6.9±2.8
5d	98	3.8±1.7	4.8±1.5	3.8±1.9	3.7±1.6	3.4±0.8
5e	95	0.9±0.4	0.8±0.5	0.7±0.3	0.7±0.2	0.5±0.1
5f	91	1.0±0.6	-	1.1±0.2	1.6±1.1	0.9±0.4
5g	86	3.5±1.2	3.9±0.9	3.4±1.5	4.6±0.7	4.4±0.6
6a	89	-	5.2±1.4	5.1±2.3	6.8±1.7	6.0±1.7
6b	93	3.5±1.5	3.9±1.8	3.8±1.4	3.6±1.5	3.9±2.6
6c	94	2.9±1.6	2.8±1.5	4.1±0.5	3.3±2.9	2.6±1.5
6d	92	3.1±0.9	4.5±0.7	4.1±2.1	-	3.9±1.6
6e	90	2.7±0.4	2.4±1.4	2.9±1.6	2.7±0.5	2.9±1.0
6f	91	1.5±0.9	1.9±0.8	1.5±1.0	1.6±0.5	1.4±0.2
6g	90	13.1±2.7	20.2±1.2	26.1±2.5	29.2±2.5	27.5±2.0
6h	83	11.4±4.1	16.5±2.7	19.6±1.6	19.2±2.1	15.8±1.8
6i	87	8.7±1.8	8.2±1.5	9.0±1.1	9.1±2.8	8.9±1.7
6j	90	6.9±2.9	6.5±2.0	-	6.2±1.2	7.7±2.5
6k	92	5.5±1.3	5.4±1.5	5.2±2.5	6.7±1.2	6.9±2.6
6l	90	4.9±1.5	4.9±3.6	5.5±2.9	5.2±1.8	7.4±8.2
6m	91	5.7±1.8	5.9±2.1	5.4±2.2	5.5±3.7	5.1±0.4
6n	92	2.2±0.6	2.4±0.7	2.5±0.7	3.1±0.9	2.6±0.9
6o	90	1.4±0.8	1.7±0.9	1.5±1.0	1.8±0.7	1.8±1.5
6p	92	3.5±1.0	-	2.9±1.2	3.3±2.0	3.9±1.4
6q	91	2.9±0.6	2.0±1.5	2.8±1.4	3.0±1.2	2.7±1.2
6r	95	1.4±0.8	1.9±0.5	1.8±0.6	1.5±0.8	1.6±0.5
6s	92	9.5±2.5	10.2±2.5	10.1±3.4	10.9±3.2	14.6±1.6
6t	88	7.2±2.2	8.5±1.2	9.9±2.6	9.8±1.4	9.0±1.7
6u	81	5.4±1.5	5.2±2.6	4.9±2.8	7.1±1.1	6.9±2.2
7b	90	0.08±0.02	0.07±0.05	0.04±0.05	0.09±0.06	-
7e	89	0.01±0.01	0.009±0.007	0.01±0.05	0.01±0.06	0.01±0.03
7f	88	0.05±0.02	0.04±0.01	0.03±0.02	-	0.05±0.07
8f	90	0.09±0.05	0.07±0.02	0.08±0.03	0.09±0.06	0.1±0.08
8o	88	0.07±0.02	0.05±0.02	0.08±0.07	0.08±0.02	0.06±0.08
8r	91	0.02±0.01	0.03±0.01	0.04±0.02	0.03±0.03	0.04±0.02

A-549 (epithelial cancer cell line): PC-3 (prostate cancer cell line): MCF-7 (breast cancer cell line): PaCa-2 (pancreatic carcinoma cell line): HT-29 (colon cancer cell line).

Table 3: Effects of selected synthetic compounds on EGFR, BRAF^{V600E}, FAK and Tubulin Polymerization and MDR reversal.

Comp.	EGFR inhibition IC ₅₀ ± SEM (μM)	BRAF inhibition IC ₅₀ ± SEM (μM)	(FAK) IC ₅₀ ± SEM (μM)	(Tubulin) Effect (arbitrary units)	Fluorescence activity ratio (FAR)
5b	1.1±0.2	1.7±0.2	7.0±1.2	410±130	55.9
5e	0.04±0.02	0.7±0.4	3.5±0.4	2930±540	67.4
5f	2.5±0.5	1.5±0.5	1.2±0.4	2580±120	59.6
6f	1.9±0.4	2.1±0.5	9.5±1.2	750±520	42.2
6o	0.06±0.05	1.0±0.2	2.4±0.7	2850±240	34.1
6r	3.1±1.2	1.9±0.7	2.0±0.2	1980±270	31.5
7b	2.4±0.5	2.3±0.5	5.5±2.2	922±180	62.2
7e	0.02±0.01	1.7±0.5	2.9±0.9	2576±190	67.6
7f	3.9±1.2	2.9±0.9	1.0±0.2	2414±520	67.9
8f	2.9±1.8	2.9±0.6	7.8±3.4	815±313	27.4
8o	0.02±0.01	2.2±0.9	1.9±0.6	2820±250	29.2
8r	4.9±1.0	3.1±0.4	1.8±0.5	2150±150	32.5
Erlotinib	0.06±0.02	0.08±0.02	7.4±1.5	-	24.7
DPBS	-	-	-	2890±285	-
Vincristine	-	-	-	713±145	-
Docetaxel	-	-	-	4995±234	-
Verapamil	-	-	-	-	12.5

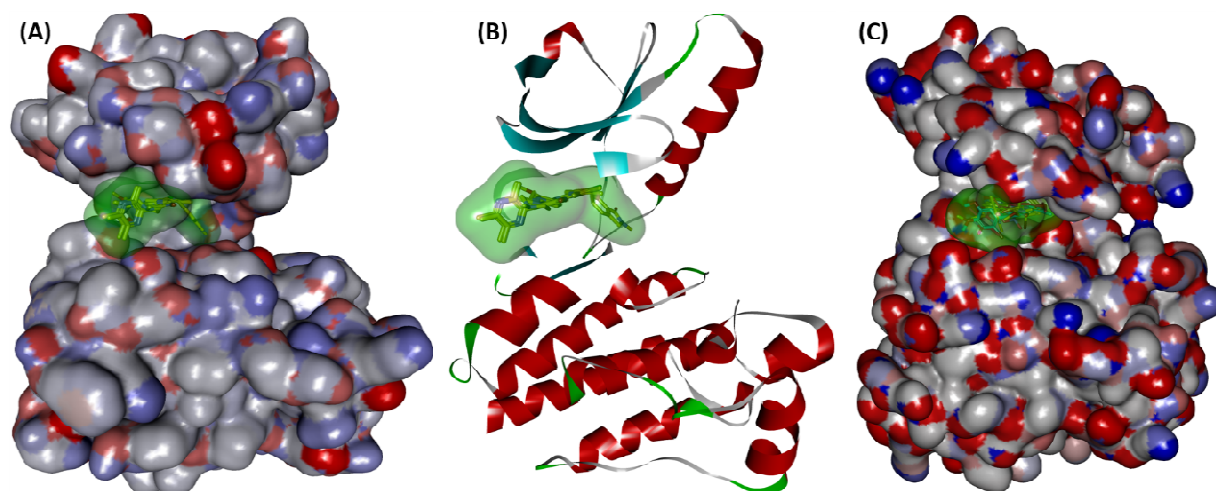


Figure 1. (A) Superimposition of the active docked poses **5f** and **7f** in addition to TAF089 inside the FAK kinase binding pocket (PDB code: 2JKO) where FAK protein is represented as a solid surface colored according to atom charges; (B) FAK protein is represented as a secondary structure (flat ribbon display style). (C) Superimposition of the active docked poses **6o** and **8o** in addition to erlotinib inside the EGFR active site (PDB code: 1M17) where EGFR protein is represented as a solid surface colored according to atom charges. The binding pockets are depicted as transparent green solid surface.

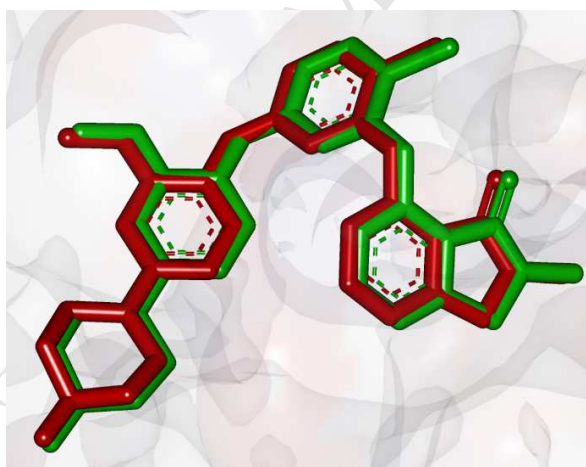


Figure 2. Comparison between the docked pose of TAF089, 7-((5-chloro-2-((2-methoxy-4-(4-methylpiperazin-1-yl)phenyl)imino)-2,5-dihydropyrimidin-4-yl)amino)-2-methylisoindolin-1-one (red) as produced by docking experiment and the co-crystallized ligand of this inhibitor within FAK kinase (green, PDB code: 2JKO).

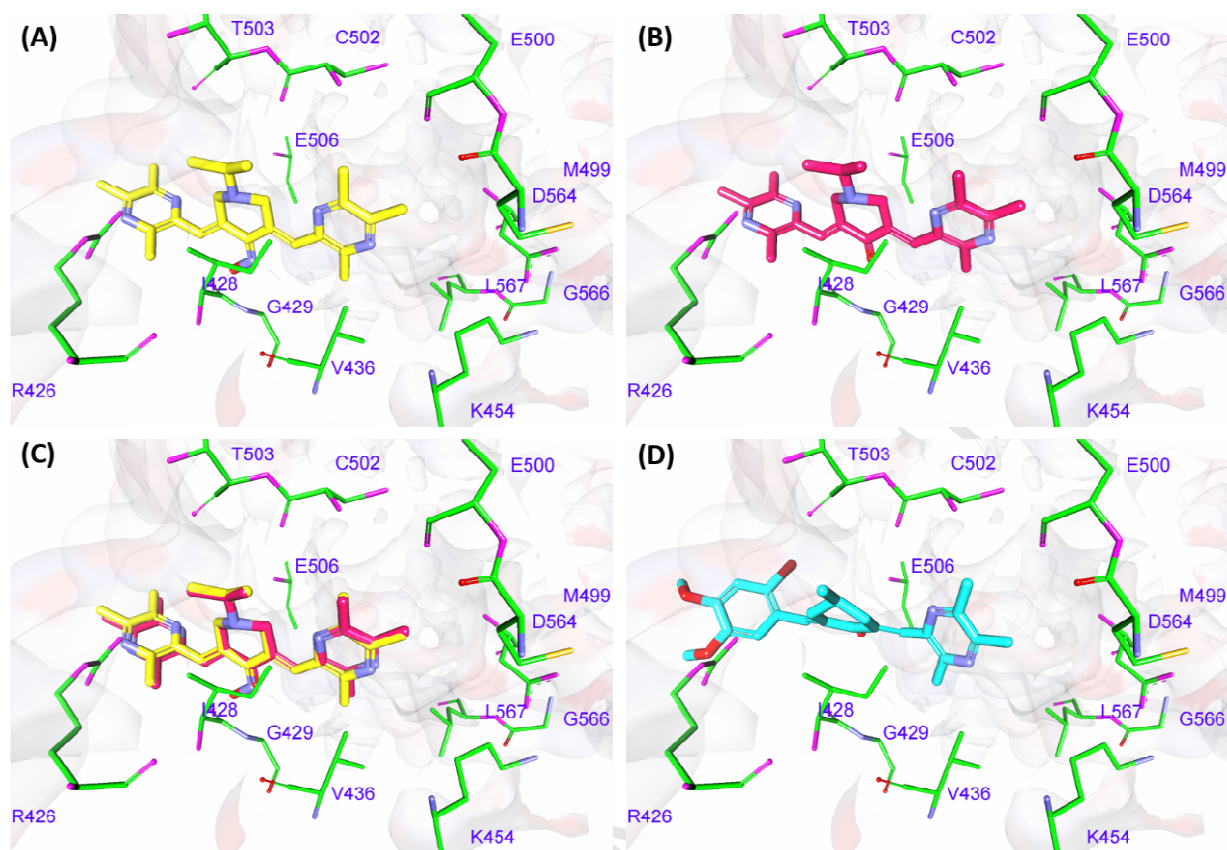


Figure 3.(A) Docking and binding pattern of compound **7f** into FAK kinase active site (PDB code: 2JKO); (B) Docking and binding pattern of compound **5f** into FAK kinase active site; (C) The superimposition of the docked pose **5f** (magenta) and **7f** (yellow) within active site of FAK kinase; (D) Docking and binding pattern of compound **6f** into FAK kinase active site. The poses were rendered as green stick models. Hydrogen bonds were represented as dashed red lines. All hydrogens were removed for the purposes of clarity.

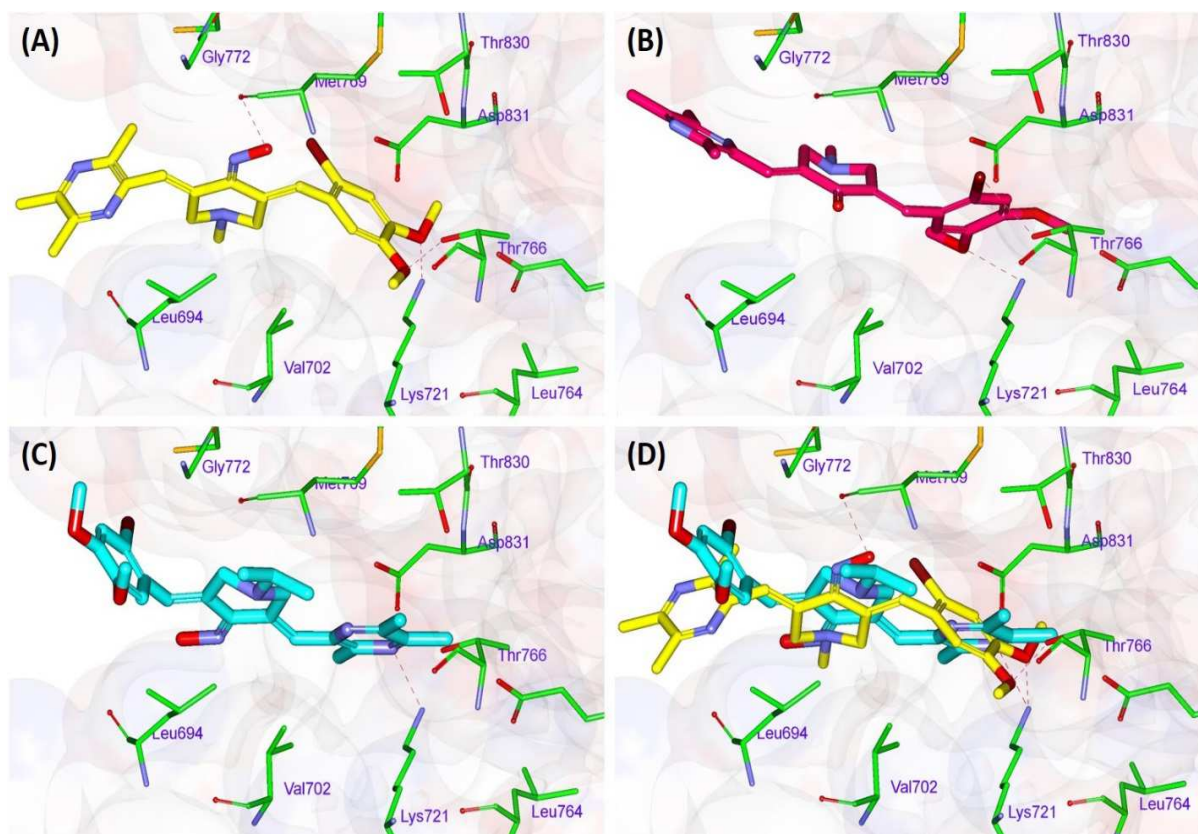


Figure 4.(A) Docking and binding pattern of compound **8o** into ATP-active site of EGFR kinase (PDB code: 1M17); (B) Docking and binding pattern of compound **6o** into ATP-active site of EGFR kinase; (C) Docking and binding pattern of compound **8r** into ATP-active site of EGFR kinase. (D) The superimposition of the docked pose **8o** (yellow) and **8r** (cyan) within the ATP-active site of EGFR kinase; The poses were rendered as green stick models. Hydrogen bonds were represented as dashed red lines. All hydrogens were removed for the purposes of clarity.

Discovery of potential anticancer multi-targeted ligustrazine based cyclohexanone and oxime analogs overcoming the cancer multidrug resistance

Gao-Feng Zha, Hua-Li Qin, Bahaa G. M. Youssif, Muhammad Wahab Amjad, Maria Abdul Ghafoor Raja, Ahmed H. Abdelazeem, Syed Nasir Abbas Bukhari

Highlights:

- New 34 ligustrazine-containing α , β -unsaturated carbonyl-based compounds and oximes are synthesized.
- All new compounds evaluated for their effects on different types of cancer cell lines.
- Most potent antiproliferative compounds are investigated for their effects on tubulin polymerization, EGFR TK kinases, KAF and BRAF^{V600E}.
- Effects on *in vitro* reversal of efflux-based resistance developed by cancer cells.
- New derivatives **5** and **7 (b,e,f)** exhibited a dual role as anticancer as well as MDR reversal agents